

This article was downloaded by:

On: 17 January 2011

Access details: *Access Details: Free Access*

Publisher *Taylor & Francis*

Informa Ltd Registered in England and Wales Registered Number: 1072954 Registered office: Mortimer House, 37-41 Mortimer Street, London W1T 3JH, UK



## Critical Reviews in Analytical Chemistry

Publication details, including instructions for authors and subscription information:

<http://www.informaworld.com/smpp/title~content=t713400837>

## Fluorescence Lifetime Imaging Microscopy (FLIM): Instrumentation and Applications

Xue Feng Wang<sup>a</sup>; Ammasi Periasamy<sup>a</sup>; Brian Herman<sup>a</sup>; David M. Coleman<sup>b</sup>

<sup>a</sup> Department of Cell Biology and Anatomy, University of North Carolina at Chapel Hill, Chapel Hill, NC <sup>b</sup> Department of Chemistry, Wayne State University, Detroit, MI

**To cite this Article** Wang, Xue Feng , Periasamy, Ammasi , Herman, Brian and Coleman, David M.(1992) 'Fluorescence Lifetime Imaging Microscopy (FLIM): Instrumentation and Applications', *Critical Reviews in Analytical Chemistry*, 23: 5, 369 — 395

**To link to this Article:** DOI: 10.1080/10408349208051651

**URL:** <http://dx.doi.org/10.1080/10408349208051651>

PLEASE SCROLL DOWN FOR ARTICLE

Full terms and conditions of use: <http://www.informaworld.com/terms-and-conditions-of-access.pdf>

This article may be used for research, teaching and private study purposes. Any substantial or systematic reproduction, re-distribution, re-selling, loan or sub-licensing, systematic supply or distribution in any form to anyone is expressly forbidden.

The publisher does not give any warranty express or implied or make any representation that the contents will be complete or accurate or up to date. The accuracy of any instructions, formulae and drug doses should be independently verified with primary sources. The publisher shall not be liable for any loss, actions, claims, proceedings, demand or costs or damages whatsoever or howsoever caused arising directly or indirectly in connection with or arising out of the use of this material.

# Fluorescence Lifetime Imaging Microscopy (FLIM): Instrumentation and Applications

Xue Feng Wang,\* Ammasi Periasamy, and Brian Herman

Department of Cell Biology and Anatomy, University of North Carolina at Chapel Hill,  
Chapel Hill, NC 27599-7090

David M. Coleman

Department of Chemistry, Wayne State University, Detroit, MI

\* Author to whom all correspondence should be addressed.

**ABSTRACT:** The new and novel techniques of fluorescence lifetime imaging (FLI)\*\* and fluorescence lifetime imaging microscopy (FLIM) provide the investigator with the capacity to quantitate two-dimensional fluorescence intensity distributions and lifetimes. The concept, theory, and instrumentation of FLI and FLIM are reviewed in this paper. The implementation of FLIM instrumentation with conventional and confocal microscopic systems is discussed. These instruments permit the quantitative measurement of molecular interactions and chemical environment from samples in biological, physical, and environmental sciences. Numerous applications in the biomedical sciences for FLIM instrumentation are also discussed.

\*\* We refer to the measurement of fluorescence lifetime images for macrosamples (e.g., cuvette) without use of a microscope as fluorescence lifetime imaging (FLI), whereas measurements obtained with a microscope are termed fluorescence lifetime imaging microscopy (FLIM).

**KEY WORDS:** fluorescence spectroscopy, time-resolved fluorescence spectroscopy, fluorescence microscopy, fluorescence lifetime imaging, time-resolved fluorescence microscopy, fluorescence lifetime imaging microscopy, confocal fluorescence microscopy, fluorescence resonance energy transfer, image intensifier, instrumentation.

## I. INTRODUCTION

Research using fluorescence spectroscopy is moving from solution spectroscopy to imaging spectroscopy.<sup>1,2</sup> In the biosciences, fluorescence imaging spectroscopy relies on fluorescence microscopy because it provides a sensitive means of acquiring information about the organization and dynamics of complex cellular structures.<sup>3</sup> Currently, most fluorescence microscopic spectroscopic measurements are performed as steady-state measurements. However, steady-state fluorescence microscopy has limited ability to study the dynamic events that may be important in cell physiology and biology for the following reasons: (1) two-dimensional (2-D) fluorescence images are usually acquired using low-speed accumulat-

ing detectors; (2) fluorescence emitted by the sample under investigation may be complex and a number of different molecular species may contribute to the overall observed signal; (3) auto-luminescence of intrinsic cellular components and scattered light;<sup>4</sup> and (4) steady-state fluorescence imaging can be difficult to quantify because there is no easy way to determine quantum yields across the sample. In contrast, time-resolved fluorescence microscopy (TRFM) allows the quantitation of dynamic and structural information from microscopic samples. This dynamic information, measured by TRFM, is very useful for understanding the interactions, binding, and associations of proteins, lipids, enzymes, DNA, and RNA.<sup>5</sup> In many cases TRFM is the only choice for studying systems that are intrinsically hetero-

geneous. Because fluorescent lifetimes are not affected by scattering or decay characteristics of the background,<sup>6</sup> measurements of fluorescent lifetimes would provide sensitive and quantitative information from the complex structure of a cell. In general, fluorescence lifetime values are more sensitive to the environment than typical spectral emission. Unfortunately, until recently, expense, complexity, and limitations in instrumentation have prevented 2-D TRFM from being performed.<sup>7</sup> Some 2-D measurements have been reported using linear array detectors or wavelength (rather than spatial) discrimination.<sup>8</sup>

Recent technological advances in laser light sources, high-speed and high-sensitive image detection devices,<sup>9</sup> fluorescence microscopy, sensitive and specific fluorescent probes for different biological molecules,<sup>10</sup> and image processing techniques have facilitated the development of fluorescence lifetime imaging microscopy (FLIM). FLIM permits the measurement of 2-D fluorescence intensity and hence, lifetime distribution, thus providing 2-D structural and dynamic information about microscopic samples.<sup>11</sup> FLIM is an extremely important advancement because it allows the combination of the sensitivity of fluorescence lifetime to environmental parameters to be monitored in a spatially defined manner in single living cells and other chemical processes.<sup>12</sup>

In this paper, the concept of fluorescence lifetime imaging (FLI) methodology is discussed; various methods (e.g., photon-counting, time-domain, and frequency-domain lifetime detection) for performing FLI measurements and its adaptation to conventional and control microscopy are included. Numerous FLIM biomedical science applications are discussed.

## II. BACKGROUND

Fluorescence has been used for a wide variety of studies because of the following features:

1. *Specificity*: fluorescent molecules absorb and emit light at specific wavelengths. Therefore, fluorescent probes can be selectively excited and detected in a complex mixture of molecular species.<sup>13</sup>
2. *Sensitivity*: small numbers of fluorescent molecules are detectable. Quantification is feasible at very low concentrations because of the inherent sensitivity associated with emission as opposed to the absorption processes. Low excitation intensities can be used to elicit a fluorescence signal, thereby preserving the viability of specimens under long-term observation.<sup>14</sup>
3. *Environmental sensitivity*: fluorescent molecules can be designed to be extremely sensitive to the immediate physical and chemical environment.<sup>15</sup>
4. *High temporal resolution*: fluorescence measurements can be used to detect very fast chemical and molecular changes in materials. Chemical and biological processes occurring on the  $10^{-12} \sim 10^{-7}$  s time scale can be detected and measured.<sup>16</sup>
5. *High spatial resolution*: fluorescence signals can be measured from cellular domains as small as single molecules if the molecules contain a sufficient number of fluorophores. Cellular components with dimensions below the diffraction-limited resolution of the light microscope can be visualized.<sup>17</sup>
6. *Three-dimensional (3-D) resolution*: 3-D chemical and biological information can be obtained with fluorescence microscopy. From conventional fluorescence microscopy, 3-D information can be estimated by the deconvolution techniques for eliminating out-of-focus information.<sup>18</sup> Confocal microscopy provides optical sections without the use of image reconstruction.<sup>19,20</sup>

Like fluorescent emission, fluorescence lifetime is an important reflection of a molecule's structure and environment, and generally falls in the range of 1 to 100 ns.<sup>21</sup> Environmental as well as competing physical processes can alter the fluorescence lifetime and provide information about the cellular milieu in which the fluorophore is located. In Figure 1, the principles of fluorescence absorption, emission, and lifetime are shown. Absorption and emission of light are illustrated by the energy-level diagram in Figure 1A. The ground, first, and second electronic states are

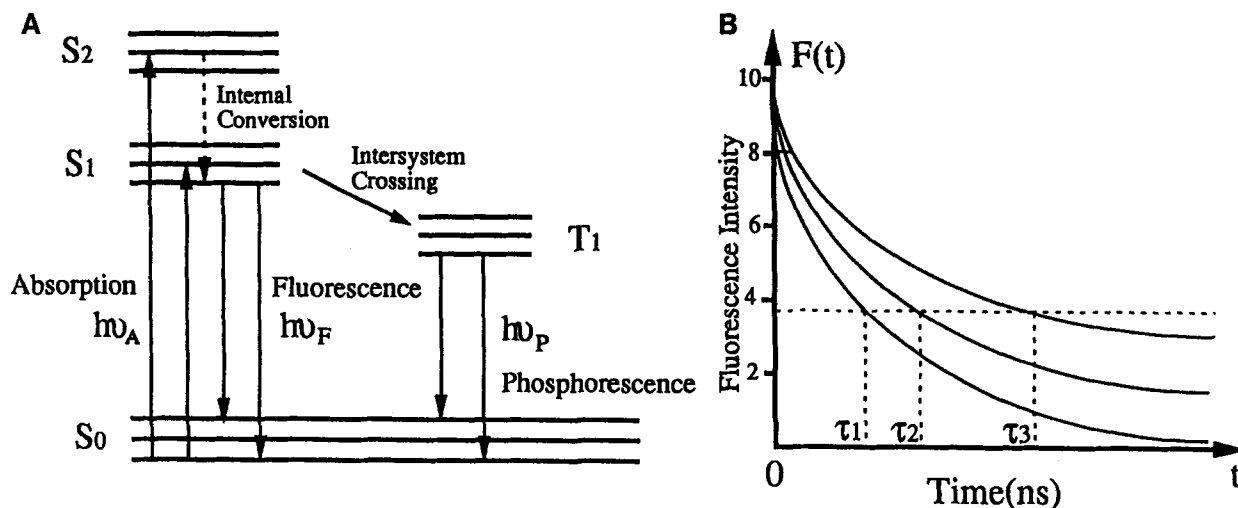


**FIGURE 1.** The energy level diagram of fluorescence process (A); and fluorescence decay and fluorescence lifetime (B).

depicted by  $S_0$ ,  $S_1$ , and  $S_2$ , respectively. Following light absorption, several processes usually occur. A fluorophore is usually excited to some higher vibrational level of either  $S_1$  or  $S_2$ . With a few rare exceptions, molecules in condensed phases rapidly relax to the lowest vibrational level of  $S_1$ . This process is called *internal conversion* and generally occurs in  $10^{-12}$  s. Since fluorescence lifetimes are typically near  $10^{-9}$  to  $10^{-8}$  s, internal conversion is generally complete prior to emission. Fluorescence emission generally results from thermally equilibrated excited states. The emissive rate of the fluorophore and the rate of radiationless decay to ground state are defined as  $\Gamma$  and  $k$ , respectively. The fluorescence lifetime is:

$$\tau = \frac{1}{\Gamma + k} \quad (1)$$

The fluorescence lifetime is the average time that a molecule remains in the excited state prior to return to the ground state. For single exponential decay fluorescence, after pulse light excitation, the fluorescence intensity with time change is described as:

$$I(t) = I_0 \cdot \exp\left(-\frac{t}{\tau}\right) \quad (2)$$

In practice, fluorescence lifetime is the time in which the fluorescence intensity decays to  $1/e$  of the intensity immediately following excitation. Typical fluorescence decay curves and fluorescence lifetime determinations for single component fluorescence are shown in Figure 1B. In practice, fluorescence decay is often multiexponential, leading to complex decay curves. Much progress has been made in analyzing and extracting multiple lifetimes from multiexponential decay curves; however, most of this work involved solution spectroscopy and very little has been performed on samples viewed through fluorescence microscopy.<sup>22</sup>

Fluorescence microscopy provides a sensitive means of acquiring information about the organization and dynamics of complex cellular structures using combinations of dyes, stains, fluorophores, or fluorophore-labeled antibodies. Recent advances in fluorescence microscopy have been made allowing quantitative measurements.<sup>23–25</sup> In order to improve spatial resolution of the fluorescence microscopy, advanced fluorescence microscopy such as confocal, total internal reflection,<sup>26</sup> and near-field fluorescence microscopy<sup>27</sup> have been introduced (see Figure 2). In conjunction with scanning and computer technology in confocal fluorescence microscopy, remarkable 2-D and 3-D images are obtained with new standards of resolution and contrast. More-

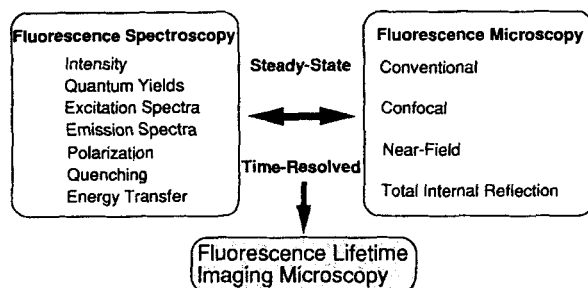


**FIGURE 2.** Fluorescence spectroscopy parameters that can be used for fluorescence microscopy. Shown is the evolution from steady-state to time-resolved fluorescence microscopy and FLIM.

over, nanometer spatial resolution has been achieved by near-field fluorescence microscopy which has potential to directly visualize DNA or protein structure.<sup>28</sup> The combination of fluorescence microscopy with fluorescence spectroscopy, intensity, excitation, and emission spectral dispersion, relative polarization, quenching, and energy transfer (in Figure 2) of steady-state prompt fluorescence has been used to generate images

and to distinguish particular molecular complexes or the local environment of labeled microscopic species. For example, in this laboratory, multi-parameter digitized fluorescence microscopy (MDFM)<sup>29</sup> is used to measure  $\text{Ca}^{2+}$ , pH, and other ion concentrations in living cells using the ratio imaging method.<sup>30–32</sup> Laser scanning confocal fluorescence microscopy is used to measure 3-D structure and function in living cells.<sup>33</sup> In clinical applications, MDFM is used for automated fluorescence image cytometry<sup>34</sup> in detection of human papilloma virus (HPV).<sup>35</sup> Digitized video fluorescence polarization microscopy was used to measure lipid order in the plasma membrane.<sup>36</sup> Plasma membrane protein and lipid lateral diffusion mobility have been measured by fluorescence recovery after photobleaching (FRAP).<sup>37</sup> MDFM also has been used to measure plasma membrane fluidity by fluorescence quenching imaging and fluorescence resonance energy transfer imaging measurements.<sup>38,39</sup>

The concept of FLIM is illustrated in Figure 3. Suppose a fluorophore in a microscopic sample exists in two distinct regions, but has a similar

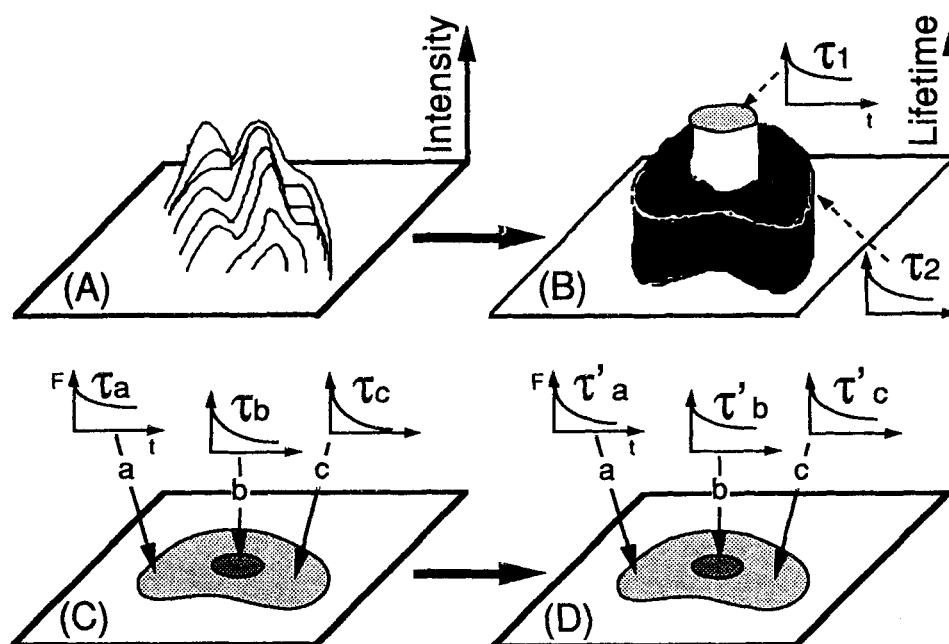


**FIGURE 3.** The concept of FLIM. Fluorescence intensity image (A) and lifetime image (B). Different lifetimes ( $\tau_1 > \tau_2$ ) in lifetime image (B) differentiate two regions in cells that are difficult to identify using intensity image (A). Fluorescence lifetime imaging changes (from C to D) are the result of changing biological or physical processes in living cells.

fluorescence intensity distribution in both regions (as shown in Figure 3A). The fluorescence lifetime ( $\tau_1$ ) at the central region of the sample is longer than that in the outer region ( $\tau_2$ ). Since the fluorophore has similar intensity distribution in the two regions, measurements of fluorescence intensity will not reveal any difference between these two regions. However, 2-D lifetime imaging would allow discrimination of the two different regions (Figure 3B). The direct visualization of a 3-D projection of the 2-D spatially dependent decay times would delineate local fluorescence lifetimes, as shown in Figure 3B. More importantly, fluorescence lifetime imaging is independent of probe concentration (up to a certain point), but is dependent on local chemical and environmental conditions. Using FLIM, it would be possible to probe specific proteins, enzymes, or DNAs, and monitor fluorescence lifetime imaging changes during some particular process (e.g., signal transduction) in living cells. Suppose that sites "a," "b," and "c" (Figure 3C and D) represent a receptor in the plasma membrane, a point in nuclear, and a point in cytoplasm, respectively. Changes in fluorescence lifetimes (between C and D) at these points provide important information concerning biophysical and biochemical mechanisms. Changes in lifetime could be caused by specific protein (e.g., receptor) conformational changes, protein-protein binding, and/or changes in pH, oxygen or calcium concentrations or conditions, which lead to quenching.

FLIM is still in its infancy. The first paper about FLIM was published in 1989.<sup>40</sup> Only a few groups in the world are working on fluorescence lifetime imaging systems.<sup>12,41–45</sup> There are two methods to perform FLIM; the first is time-domain FLIM using photon counting and gating methods;<sup>46,47</sup> the second is frequency-domain FLIM using phase-resolved and multifrequency modulation methods.<sup>15,48</sup> The relative merits of the two methods have long been debated in the fluorescence spectroscopic community. An alternative hybrid implementation, comprising modulated excitation and a modified imaging photon detector coupled to a custom built photon correlator, has also been described.<sup>49</sup> Fluorescence lifetime imaging systems in the laboratory using both methods have been evaluated.<sup>40,41,45,50</sup> Each

approach has its advantages and disadvantages, depending mainly on the biological events to be monitored and microscopic techniques used in the experiments.

### III. FLUORESCENCE LIFETIME IMAGING SYSTEMS

The determination of fluorescence lifetimes is traditionally carried out by two techniques: (1) time-domain pulse methods<sup>46,47</sup> and (2) frequency-domain or phase-resolved methods.<sup>15,48</sup> A functional representation of fluorescence lifetime measurements is outlined in Figure 4. In time-domain methods, using pulsed light excitation, lifetimes are measured from the fluorescence signal directly or from photon counting detection. In the frequency-domain or phase-resolved method, with sinusously modulated light excitation  $E(t)$ , lifetimes are determined from phase shift  $\Phi$  or modulation depth  $M_F$  of the fluorescence emission signal. There are number of commercial lifetime measurement instruments available using time or frequency domain methods (see Table 1) for single point measurements. It is possible to measure fluorescence lifetime images by combination of the lifetime determination (time- and frequency-domain) techniques with high-speed 2-D detectors and scanning techniques such as mechanical

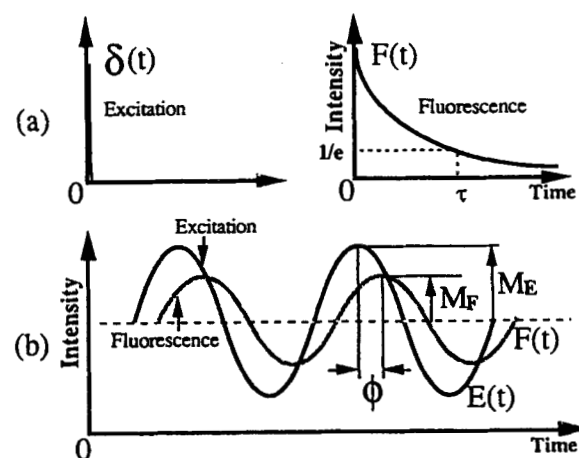


**FIGURE 4.** Fluorescence lifetime determination methods: (a) time-domain pulse method (impulse response); (b) frequency-domain phase-resolved method (frequency response).

**TABLE 1**  
**Commercial Lifetime Measurement Instrumentation**

Model	Characteristics	Company
LS 100 Series luminescence spectrophotometer	Wavelength: 200–930 nm Light source: xenon lamp PC-based system Collection time for single- and two- component are 15 min and 1.5 h, respectively	Photon Technology International, Inc., South Brunswick, NJ
SPF-500c and 4800 series spectrophotometer	Wavelength: 200–900 nm Light source: xenon lamp or lasers PC-based system Collection time: 1 ms per data point PMT R928P or MCP-PMT	SLM Instruments, Inc. Urbana, IL
Fluorescence lifetime systems; different models depending on temporal resolution and applications	Wavelength: 180–950 nm Light source: coaxial flash lamp or lasers Rep rate: 100 KHz PMT, MCP-PMT, and single- photon avalanche diode cooling system available for the detectors	Edinburgh Instruments Canada
Multifrequency cross- correlation phase & modulation fluorometer, ISS K2 series	Wavelength: 380–670 nm Light source: xenon arc lamp or lasers Lifetime measurement range from 10 ps to 1 $\mu$ s PC-based system Hamamatsu side-on selected PMT	ISS Inc., Champaign, IL

stage scanning, laser beam scanning, or electronic (e.g., image dissector or streak camera) scanning methods.<sup>51</sup>

## A. Photon Counting Mode

In fluorescence spectroscopy, it is necessary to minimize the intensity or vary the duration of light illumination to the sample (especially for living samples) to reduce the effects of photochemical reaction and photobleaching. Fluorescence emission intensity depends on the intensity of excitation light and concentration of the fluorophores under study. For low-intensity excitation, fluorescence emission would be weak. Time-resolved fluorescence measurements on the nanosecond level would reduce further the fluorescence emission. For the detection of a very low-light level signal on a nanosecond time scale, photon-counting techniques are required.<sup>52</sup>

## 1. Single Photon Counting (SPC)

Time-correlated SPC techniques are currently the most widely used methods for measuring weak fluorescence decay times.<sup>47</sup> Historically, SPC has been performed using air-gap arc flash lamp excitation sources and conventional photomultiplier tube (PMT) detection; however, the time required to collect sufficient data for accurate lifetime measurements has precluded studies of dynamic events. Two developments have brought about radical improvement in the time resolution of SPC fluorescence lifetime measurements: (1) the use of picosecond ultrafast tunable dye lasers as excitation sources and (2) the development of the microchannel-plate photomultiplier tube (MCP-PMT),<sup>53,54</sup> which has the advantages of wide dynamic range ( $10^6$ ), single photon sensitivity, and high time resolution (10 ps).<sup>55,56</sup> The principle of SPC is based on the repetitive measurement of the time interval between the pulsed excitation and

the formation of a single photoelectron at a detector. In practice, SPC systems consist of a timing discriminator, a time-to-amplitude converter (TAC), and a multichannel pulse height analyzer. It repetitively accepts the excitation-emission pulse pairs, measures their time intervals, and then records each event in a memory location corresponding to the time interval between the excitation pulse and the first recorded emitted single photon. The characteristics of the detectors in SPC (shown in Table 2) are important. It should have excellent time response, short rise time, and transit time spread (TTS); it also must have the ability to count single photons with low dark noise and high sensitivity. The PMT time response to impulse excitation should have a low dependency on the wavelength of incident light.

In most current SPC instruments, an MCP-PMT is used due to the short transit time spread, low dark count, and independence of detection efficiency on emission wavelength. It is possible to undertake fluorescence lifetime imaging by combining SPC and scanning techniques. However, for measurements of dynamic events, problems could arise due to the long measurement time involved in collecting the photons at each point.

## 2. Multichannel Photon Counting (MPC)

According to the principle of the SPC technique, one photon is detected for each excitation. This low counting efficiency results in a long observation time for mapping 2-D samples. In

**TABLE 2**  
**Typical Characteristics of MCP-PMT Used in SPC**

Company and product	Gain	Risetime (ns)	Transit time spread (ns)	Spectral range (nm)	Cathode sensitivity luminous type ( $\mu\text{A/lumen}$ )
Hamamatsu (MCP-PMT) R1564U, Bialkali 2 stage MCP anode to cathode supply voltage 3000 (Vdc)	$5 \times 10^5$	0.22	0.070	300–650	50
Hamamatsu (MCP-PMT) R 2808U, Bialkali 2 storage MCP anode to cathode supply voltage 3000 (Vdc) dark count 1000 cps at 25°C	$5 \times 10^5$	0.15	0.055	300–650	50
Hamamatsu (MCP-PMT) R 2566U, Bialkali 2 storage MCP anode to cathode supply voltage 4000 (Vdc) dark counts 500 cps at 25°C	$5 \times 10^5$	0.1	—	300–650	50
Burle Instruments PMT-8852, dark current 2-in. diameter 12 stages magnetic shield required supply voltage 2500 (Vdc)	$6 \times 10^5$	2.4	0.34	400–900	115
Burle Instruments PMT-7764, dark current 3NA 1.9-diameter 6 stages magnetic shield required supply voltage 1500 (Vdc)	$0.01 \times 10^6$	1.5	13	300–660	40



many experiments, it is desirable to decrease observation times by increasing the acceptable number of photoelectron pulses per excitation. Rapid measurement of 2-D samples has important ramifications in biomedical research. For this purpose, MPC with high sensitivity and good counting efficiency was developed.<sup>45,57,58</sup> This technique drastically reduces measurement time. In short, all photons in an energy burst (fluorescence emission) are sampled simultaneously such that time information is preserved. A corresponding reduction in measurement time makes 2-D lifetime mapping practical.<sup>47</sup> Compared with SPC detection, MPC reduces measurement time and improves the signal-to-noise ratio (SNR) by over two orders of magnitude. In Figure 5, a comparison of the operation of MPC and SPC is shown. For one excitation, there are three fluorescence photons. Using the SPC method, the first pulse (a) is the stop pulse for the TAC; therefore, information from only one pulse is recorded in memory. In contrast, the MPC method counts all photons (a, b, and c) simultaneously, providing higher counting efficiency and shorter observation time.

Two types of the MPC fluorimetric systems have been developed. The first one is the system using two units of high-speed ECL shift registers in which all fluorescence photons are sampled simultaneously and recorded.<sup>47</sup> Using this MPC system in conjunction with stage scanning, microscopic lifetime imaging measurements were carried out. The second MPC fluorimetric system

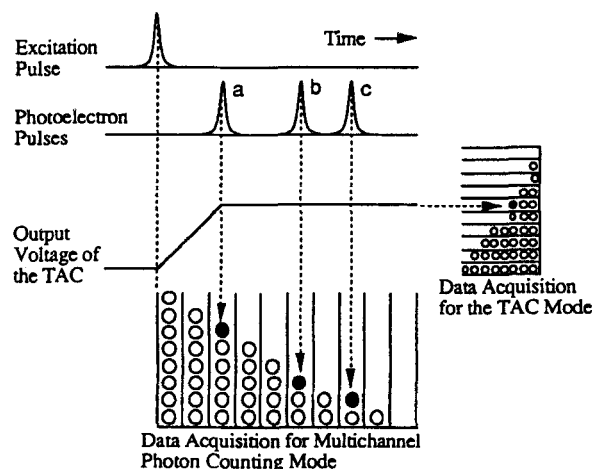


**FIGURE 5.** A comparison of the operation of multichannel and single photon counting modes.

uses optical fiber dynamic memory based on the vernier chronotron technique.<sup>58</sup> In this approach, two single-mode optical fiber loops in conjunction with pulsed laser diodes and avalanche photodiodes (APD) were used. The extremely low loss, good linearity, and large available time-bandwidth of single-mode fiber allow signals to propagate large distances without significant attenuation or distortion, so that good stability and high-resolution measurements are possible. However, neither of these MPC techniques provides the required temporal resolution to study cellular dynamics. This problem can be solved by using high-speed, 2-D image detectors.

## B. Time-Domain FLI

New advances in image intensifier detector techniques allow time gating to a few nanoseconds or even subnanoseconds.<sup>59,60</sup> The principal features of the gated image intensifier are very small image distortion, wide spectral response, compact size, high sensitivity, high gain, and high spatial resolution.<sup>9</sup> A functional description of the gated image intensifier-CCD combination is shown in Figure 6. In the gated operation mode, the photocathode of the intensifier is biased to a cut-off positive potential (+150 V) relative to the MCP-In potential, while keeping  $V_{MCP}$  and  $V_S$  at their normal operating potentials. When a high negative (−300 V) gate pulse is applied on the photocathode, an intensified image can be ob-

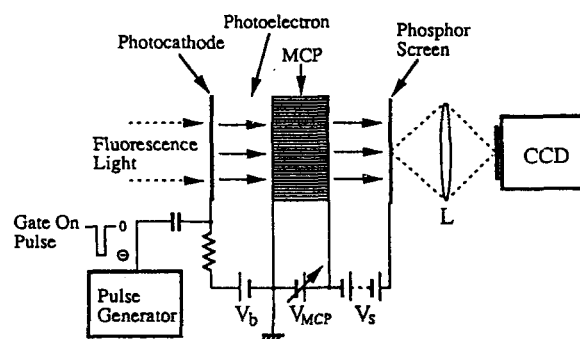


**FIGURE 6.** Functional description of the gated intensifier-CCD combination. For gated operation,  $V_b$ : 150 V;  $V_S$ : 5500 V; and  $V_{MCP}$ : 500 to ~900 V depending on the required gain.

served on the phosphor screen. The phosphor screen luminance is typically around  $4 \times 10^{-2}$  ft-L for a 100-ns gate time. The output image of the intensifier on the phosphor screen is focused at unity magnification onto a CCD camera. For weak fluorescence emission, the target integration in the CCD is effective at enhancing SNR of detected images. In a given situation, the available fluorescence light level determines the integration time required to obtain acceptable SNRs. Cooling the CCD to reduce dark current to negligible levels permits long integration times. High-speed image intensifiers available with different gating times are listed in Table 3. An FLI system using a gated MCP image intensifier (time resolution: 2.5 ns) coupled to a CCD camera has been developed.<sup>41</sup> Using a rapid lifetime determination method for multigate detection, fluorescence lifetime images were obtained quickly.

A functional description of the FLI system using a gated MCP image intensifier is shown in Figure 7. In the gated mode, the time-resolved fluorescence image of the sample at  $t_d$  is obtained by applying a sampling gate pulse (duration  $\Delta T$ ) to the photocathode of the intensifier at time  $t_d$  following sample excitation. Several sampling time positions can be selected during the fluorescence decay (i.e., multigate detection). Using rapid lifetime computational procedures for multigate detection, fluorescence lifetime imaging can be derived. Various methods for analysis of fluorescence decay data have been proposed. For 2-D measurements, however, using conventional methods, extracting parameters  $A$  and  $\tau$  from an enormous number of data points is tedious. For a single exponential decay of the fluorescence signal excited by a short-duration pulsed light source described in Equation 1, fluorescence decay can be detected at two different delay times,  $t_1$  and  $t_2$ ,

**TABLE 3**  
**Cameras Used in Lifetime Imaging Systems**

Model	Characteristics	Company
High-speed gated image intensifier, Model c2925 Single-stage MCP	Wavelength: 180–840 nm Rep Rate: 10 KHz Gating: 3 ns–100 ns (continuously variable) Rise and fall time: 2 and 3 ns Gating jitter: 200 ps max. Cathode sensitivity: 150 $\mu$ A/lumen Quantum efficiency: 13%	Hamamatsu Corporation, Bridgewater, NJ
Proximity focused channel intensifier tubes, F4111 Series single-stage MCP	Wavelength: 450–550 nm Rep Rate: 10 KHz (Avetech Electronics) Gating: 2 ns–10 ms Rise and fall time: 2 to 10 ns Cathode sensitivity: 225 $\mu$ A/lumen Resolution range: 22–26 line pairs/mm	Electro Optical Products Division, ITT, Fort Wayne, IN
Image intensifier Model ICCD-576 single-stage MCP Gatable ICCD	Wavelength: 120–920 nm Rep Rate: 5 KHz Gating: 6 ns to few ms Wavelength: 180–840 nm Rep rate: 5 KHz Gating: 5 ns to few ms	Princeton Instruments, Inc., Trenton, NJ  Photometrics, Ltd., Tucson, AZ
Ultra high-speed ICCD cameras	Wavelength: 130–920 nm Gating: 5 ns to DC Sensitivity: 1 count/3 photoelectrons/ pixel at 50-ns gate width Cooled option available (modulation range up to 600 MHz)	Stanford Computer Optics, Palo Alto, CA

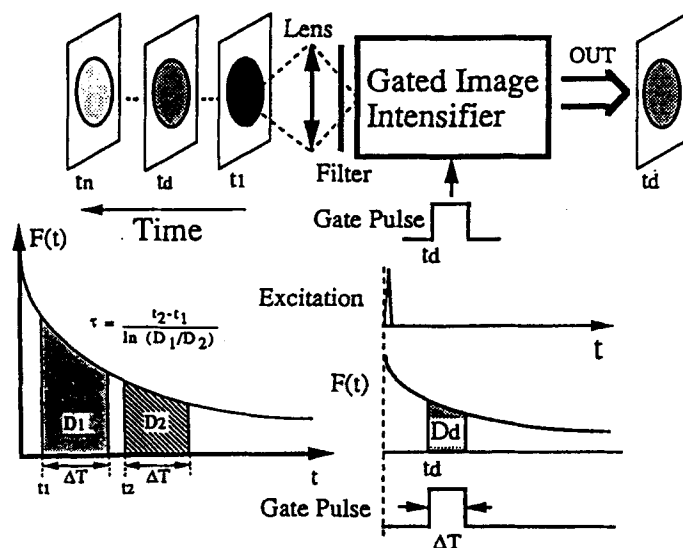


**FIGURE 7.** Functional description of time-resolved fluorescence image detection using a gated image intensifier and representation of rapid lifetime determination for a single exponential decay.

with gate width  $\Delta T$ . The gated fluorescence signals ( $D_1$  and  $D_2$ ) can be described as:

$$D_1 = \int_{t_1}^{t_1 + \Delta T} A \cdot \exp(-t/\tau) dt \quad (3)$$

$$D_2 = \int_{t_2}^{t_2 + \Delta T} A \cdot \exp(-t/\tau) dt \quad (4)$$

The lifetime  $\tau$  and pre-exponential factor  $A$  can be extracted as follows:

$$\tau = \frac{t_2 - t_1}{\ln(D_1/D_2)} \quad (5)$$

$$A = \frac{D_1}{\tau \cdot \exp(-t_1/\tau) \cdot [1 - \exp(-\Delta T/\tau)]} \quad (6)$$

The lifetime is dependent on the ratio of  $D_1/D_2$  and the selection of  $t_1$  and  $t_2$  time points; it is not dependent on the gated image intensifier time resolution (2.5 ns). The ratio term of  $D_1/D_2$ , which makes lifetime calculation independent of fluorescent dye concentration, is an important

feature for the applications such as cellular lifetime imaging. Use of this method also results in extremely short calculation times. Fluorescence lifetimes and pre-exponential factors can be calculated directly from only four parameters ( $D_1$ ,  $D_2$ ,  $t_1$ , and  $t_2$ ) without fitting a large number of data points as is required by conventional least-squares methods.<sup>47,61</sup> With a gated intensifier for multigate detection, both the observation time and the calculation time can be reduced.

FLI system performance using a gated image intensifier has been evaluated. Fluorescence lifetime imaging of a well-characterized single standard sample (1 ppm quinine sulfate in 0.1 M  $H_2SO_4$ ) was determined. A quartz cell was used for these measurements. For the experiments, the  $N_2$  laser operated at 25 Hz; the integration time of the CCD camera was 1 s. Therefore, 25 fluorescence images were integrated at the target of the CCD camera. After sample excitation, two gated fluorescence intensity images ( $128 \times 128$ ) of quinine sulfate at gate time  $t_1 = 1$  ns and  $t_2 = 5$  ns were detected as shown in Figure 8. The gate width,  $\Delta T$ , of the gated image intensifier was set at 10 ns. Since only 1 s is required, this method is considerably faster than previously reported methods. At room temperature, detection is rather noisy.

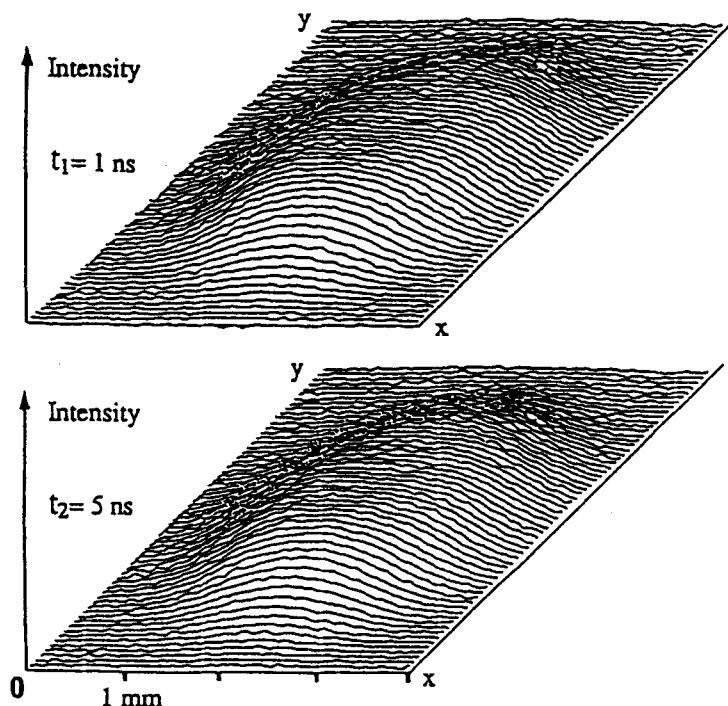


**FIGURE 8.** Time-resolved multigate fluorescence image patterns ( $128 \times 128$ ) of a standard sample (1 ppm quinine sulfate in 0.1 M  $\text{H}_2\text{SO}_4$ ) at  $t_1 = 1$  ns and  $t_2 = 5$  ns after pulsed light excitation.

Therefore, background noise of the intensifier and the CCD camera also was measured to derive the pure signal components. Fluorescence lifetime imaging calculated from these images is shown in Figure 9. Calculation time for this lifetime imaging data was 4 s. The average lifetime of quinine sulfate was calculated as 19.2 ns. This compares favorably with accepted values (19.4 ns) with the use of a pulse-sampling oscilloscopic technique.<sup>62</sup>

## C. Frequency-Domain FLI

### 1. FLI System Using an Image Dissector Tube

In frequency-domain phase-modulation methods, high-frequency (MHz to GHz) sinusoidally modulated radiation is used to excite the sample. Following excitation, fluorescence lifetimes are determined from phase shifts or amplitude demodulation factors. In recent years, phase-resolved fluorescence spectroscopic methods for multicom-

ponent measurements have been established.<sup>63,64</sup> The frequency-domain methods, when combined with high speed 2-D detectors, can measure temporal, spatial, and wavelength-resolved information simultaneously.

A 2-D image dissector tube (IDT) has been used as a detector for frequency-domain FLI.<sup>40</sup> The principal features of this device are (1) nonstorage random scan operation, (2) fast response, (3) low dark current, (4) wide dynamic range, (5) linear input-output characteristics, and (6) high spatial resolution. IDT operation is based on the use of electron beam scanning. The optical image formed on the IDT photocathode produces a cloud of photoelectrons that is focused by a coil onto a plate having a small central hole (dissecting aperture). Only those electrons that are aligned with the aperture pass through and are multiplied at high gain, as in a PMT, to produce an output current at the anode. A set of X and Y deflection coils scans the entire electron cloud in a raster pattern so that photoelectrons that are aligned with the aperture come

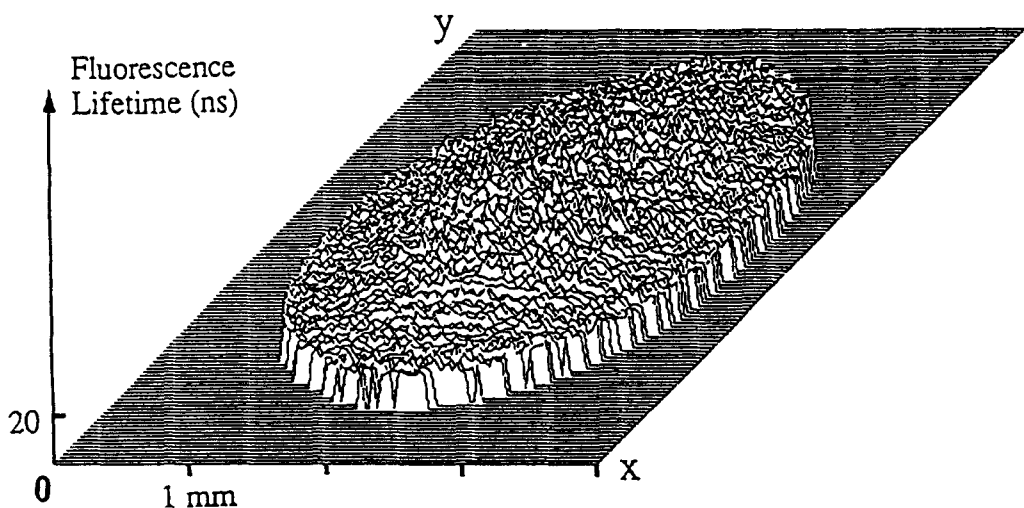


**FIGURE 9.** Fluorescence lifetime imaging of standard sample (1 ppm quinine sulfate in 0.1  $M$   $H_2SO_4$ ).

from sequentially different parts of the original image at the faceplate.

When the sample under study is excited with time-dependent sinusoidally modulated light  $E(t)$ ,

$$E(t) = A[1 + M_e \cos(\omega t)] \quad (7)$$

(where  $A$  is the DC intensity component of the exciting light,  $\omega = 2\pi f$  and  $f$  is the modulation frequency, and  $M_e$  is the ratio of the amplitude of the AC intensity to the DC intensity component). The resulting wavelength-dependent fluorescence  $F(\lambda, \tau)$ , for a single component sample with exponential decay, will have frequency  $f$  but will be phase shifted by an angle  $\Phi$ , which is unique to the particular fluorescent species, that is,

$$F(\lambda, t) = A'(\lambda)[1 + M_f \cos(\omega t - \Phi)] \quad (8)$$

where  $A'(\lambda)$  is the average fluorescence intensity. The phase shift  $\Phi$  and the modulation factor  $M$  are related to the fluorescence lifetime  $\tau$  by:

$$\tan \Phi = \omega \tau \quad (9)$$

$$M = M_f / M_e = 1 / [1 + (\omega \tau)^2]^{1/2} \quad (10)$$

Phase-resolved measurements using heterodyne detection<sup>65</sup> are accomplished by modulating the

gain of the IDT with a sinusoidal reference signal at the IDT blanking electrode whose frequency  $f_r$  is slightly different from  $f$  ( $\Delta f$  smaller than  $f$ ). The gain of the IDT is:

$$G_r = G_0 + G_1 \cos(\omega_r t) \quad (11)$$

Heterodyne detection multiplies the fluorescence emission  $F(\lambda, \tau)$  by the gain of the IDT. The output photocurrent  $I_o(t)$  of the IDT is given as:

$$I_o(t) = A'(\lambda) \left\{ G_0 + \frac{1}{2} M_f G_1 \cos[(\omega - \omega_r)t - \Phi] + G_1 \cos(\omega_r t) + G_0 M_f \cos(\omega t - \Phi) + \frac{1}{2} M_f G_1 \cos(\omega t + \omega_r t - \Phi) \right\} \quad (12)$$

When  $\omega_r \approx \omega$ , Equation 12 can be simplified by a DC component,  $\Delta\omega$  ( $= 2\pi\Delta f$ ) term, and a high-frequency term. The high-frequency terms are electronically filtered out leaving the DC and  $\Delta\omega$  terms:

$$I_j(t) = A'(\lambda)G_0 + \frac{1}{2} A'(\lambda)M_f G_1 \cos(\Delta\omega t - \Phi) \quad (13)$$

The DC term  $A'(\lambda)G_0$  contains the fluorescence intensity information. The AC term contains the phase and modulation information that is necessary to determine fluorescence lifetimes. Fluores-

cence lifetimes are determined from the phase shift  $\Phi$ . A functional description of heterodyne detection using IDT is shown in Figure 10. The interrelationship between the aforementioned signals is shown for the measurement of one fluorescent data point. A reference signal  $I_r(t)$  of frequency  $\Delta f$  is used for phase shift  $\Phi$  detection.

When the fluorescence spectra of two components are nearly identical, it may be difficult to differentiate between them. In such cases, fluorescence lifetime differences can be used to accentuate differences in spatial distribution. The fluorescence spectrum of two samples of acridine orange and uranine are shown in Figure 11A. It can be seen that their spectra are very similar, but that their fluorescence lifetimes are quite different. An FLI for these fluorescence samples is shown in Figure 11B. The two samples are each placed on a slide glass and are fixed in circular shapes. Based on different fluorescence lifetimes, the center is uranine ( $\tau = 6.9$  ns), while the outside is acridine orange ( $\tau = 4.9$  ns).

Frequency-domain FLI also can be used for enhancing image contrast. For example, by varying the phase of the reference signal  $\Phi_D$ , can one spatially separate the lifetimes of the two components (Figure 12). There is acridine orange and uranine in the sample. The fluorescence spectrum of the two components is identical, as shown in Figure 11. Using the phase-resolved method, the

output of the phase-resolved detection for the two component samples is

$$I_0 = I_a(\lambda) \cos(\Phi_D - \Phi_a) + I_b(\lambda) \cos(\Phi_D - \Phi_b) \quad (14)$$

where  $\Phi_a$  is the phase shift related to the lifetime of acridine orange (a) and  $\Phi_b$  is the phase shift related to the lifetime of uranine (b). Based on the FLI system using an IDT, Figure 12A shows the result for a two-component distribution measurement where reference signal phase  $\Phi_D$  is not same as  $90^\circ + \Phi_a$  or  $90^\circ + \Phi_b$ . On the right is acridine orange (a), the left is the uranine (b), and the wavelength of the monochromatic filter was set at 550 nm. When the  $\Phi_D = 90^\circ + \Phi_a$ , from Equation 14, it can be seen (B) that only the uranine (b) fluorescence component was measured. In Figure 12C, when the  $\Phi_D = 90^\circ + \Phi_b$ , only acridine orange (a) lifetime is measured. Using a frequency-domain FLI system, one can spatially separate based on lifetime measurements the components of a mixed fluorophore population.

## 2. FLI System Using a Homo- or Heterodyne Image Intensifier

Similar to an image dissector tube, the high-speed intensifier gain can be modulated by an RF

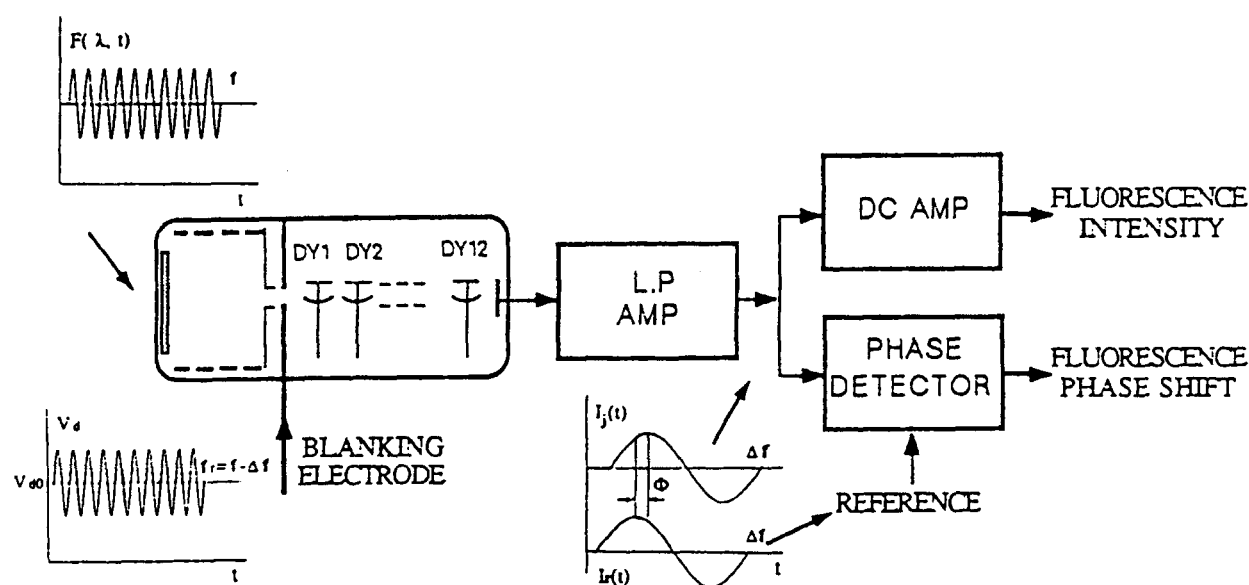
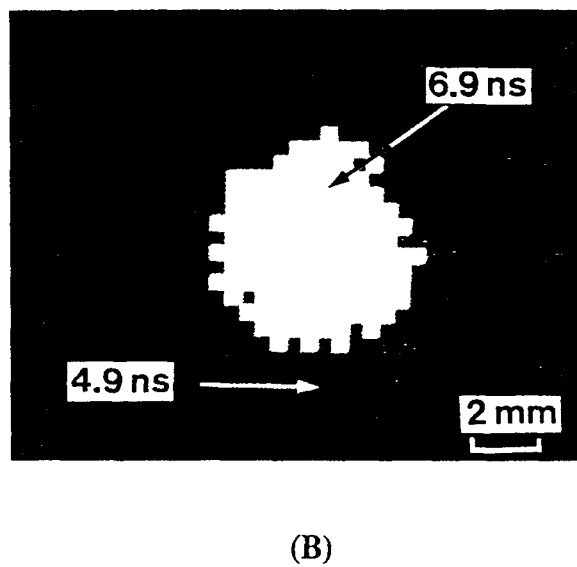
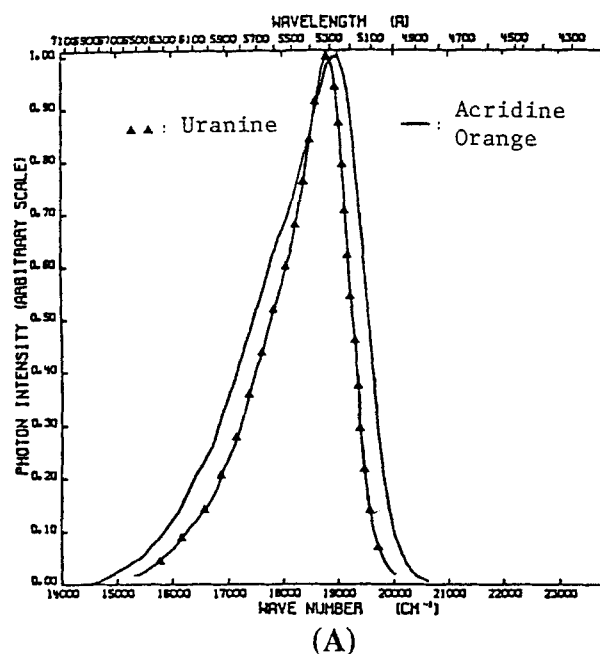


FIGURE 10. Functional description of heterodyne detection system in the image dissector tube.



**FIGURE 11.** (A) Fluorescence spectra of acridine orange and uranine; (B) fluorescence lifetime imaging of these two components with similar spectra. Center is uranine ( $\tau = 6.9$  ns), while the outside is acridine orange ( $\tau = 4.9$  ns).

signal applied between the photocathode and microchannel plate (MCP) input surface. By combining a CCD camera and image intensifier, high-frequency gain-modulation of an image intensifier at the same frequency as the light modulation frequency (homodyne detection), or at some harmonic of the laser repetition rate, can be used to create lifetime images. An FLI system has been developed by combining a homodyne image intensifier and slow-scan CCD camera.<sup>66</sup> The light source was a mode-locked Antares Nd:YAG laser, frequency doubled to 532 nm at a 76.2-MHz repetition rate. The fundamental or second harmonic of the pulse train, at 152.4 MHz, was used for lifetime measurements. The image intensifier was used as a 2-D phase-sensitive detector in which the signal intensity at each position ( $r$ ) depends on the phase angle difference between the emission and the gain modulation of the detector. This results in a constant intensity that is proportional to: (1) the concentration of the fluorophore ( $c$ ) at location  $r$  [ $C(r)$ ]; (2) the cosine of the phase angle difference; (3) the extent of modulation of the detector; and (4) the modulation of the emission at each location [ $m(r)$ ],

$$I(\Phi_D, r) = kC(r) \left[ 1 + \frac{1}{2} m_D m(r) \cos\{\Phi(r) - \Phi_D\} \right] \quad (15)$$

In this expression,  $\Phi_D$  is the phase of the gain-modulation and  $\Phi(r)$  is the phase angle of the fluorescence. A value of  $\Phi_D = 0$  results in maximum intensity for a zero lifetime, that is, scattered light. The homodyne measurements are performed electro-optically on the high-frequency modulated emission. The phase angle of the fluorophore is related to the apparent phase lifetime  $\tau_F$  and the modulation frequency ( $\omega$  in radians/s) by

$$\tan \Phi(r) = \omega \tau_F(r) \quad (16)$$

Using this method, it is not possible to calculate the lifetime from a single phase-sensitive intensity. However, by varying  $\Phi_D$ , it is possible to determine  $\Phi(r)$ . After collecting a series of phase-sensitive images, in which  $\Phi_D$  is varied over 360°, the phase-sensitive intensities at each pixel are used to determine the phase and modulation at each pixel, resulting in the phase angle, modulation, or lifetime images. The data sets for the FLI are rather large, resulting in time-consuming data

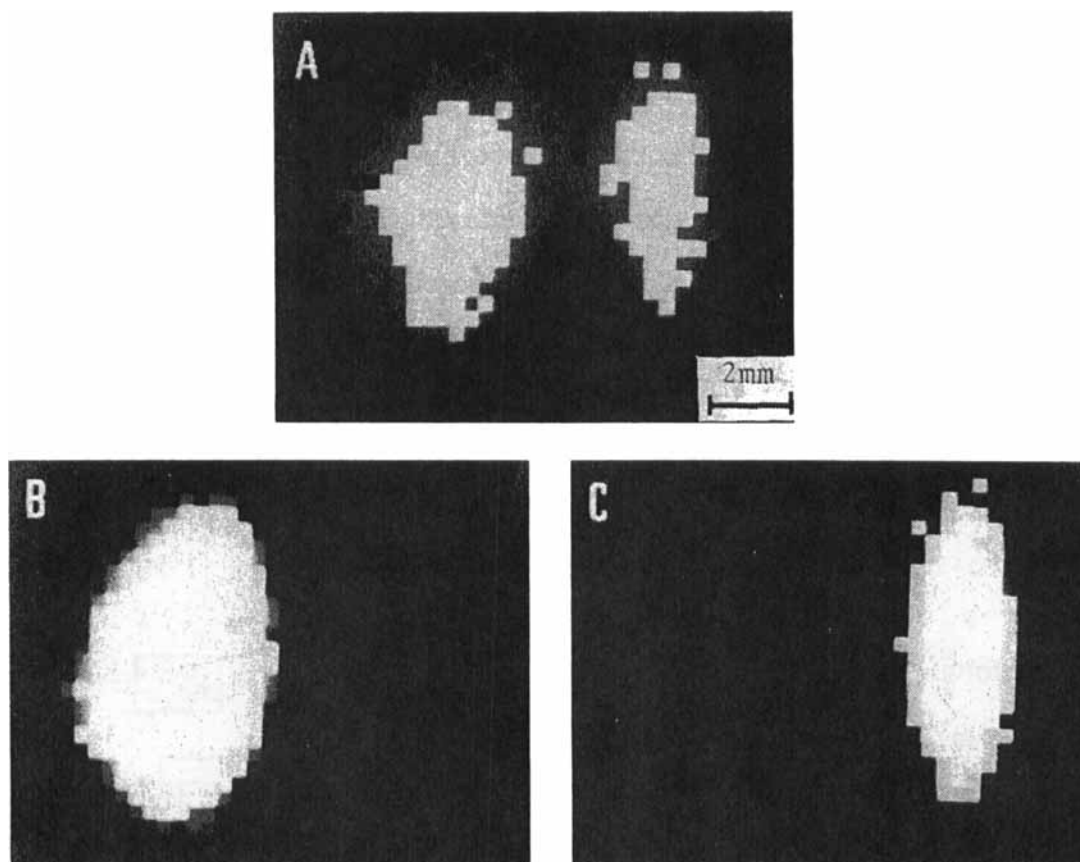


**FIGURE 12.** A two-component fluorescence pattern (A) of acridine orange (right) and uranine (left). The two-component fluorescence distribution was separated by using a phase-resolved method. (B) The distribution of uranine; (C) the distribution of acridine orange.

storage, retrieval, and processing. To allow for more rapid image processing, an algorithm to calculate the phase and modulation images needs to be developed.

Table 4 compares different FLI system features. It is necessary to consider detection sensitivity, time resolution, lifetime image formation, and lifetime imaging time to design an FLI system.

#### IV. FLUORESCENCE LIFETIME IMAGING MICROSCOPY

Most spectroscopic studies using fluorescence microscopy have centered around measurements of fluorescence spectra, excitation spectra, and polarization, all using continuous

wave (CW) illumination. Little attention has been paid to time-resolved fluorescence microscopy in which the lifetime of fluorochromes is sought. Fluorescence lifetime information, with the additional spatial resolution that the microscope provides, allows 2-D or 3-D information relevant to dynamic cell component interactions to be obtained. In addition, stray light and background luminescence arising from the samples or the optical system are easily discriminated with the time-resolved method.<sup>7,67</sup> However, most instrumentation used for fluorescence lifetime measurements through a microscope use spot photometric detection. Because only a small portion of a cell (a "spot") can be examined at any one time, these instruments do not provide high temporal or spatial resolution lifetime images.



**TABLE 4**  
**Comparison of Different FLI System Features**

	Sensitivity (gain)	Time resolution	2-D formation	FLI time	Photo- bleaching
Single photon counting (SPC)	$10^6$	10 ps	Scanning	Longest	Lowest
Multichannel photon counting	$10^6$	>0.2 ns	Scanning	Long	Low
Gated image intensifier	$10^4$	2.5 ns	Nonscanning	Shortest	Low
Image dissector	$10^5$	<0.1 ns	Electron beam scanning	Short	High
Heterodyne image intensifier	$10^4$	<0.1 ns	Nonscanning	Long	Higher

### A. Conventional FLIM

Conventional FLIM is based on the combination of time- and frequency-domain FLI with conventional fluorescence microscopy. Using pulsed or modulated Kohler excitation, time-resolved fluorescence emission images can be obtained using high-speed image detectors (e.g., gated image intensifier, image dissector tube). An FLIM using a gated image intensifier is shown in Figure 13. The major components are (1) the excitation source; (2) a fluorescence microscope; (3) a time-resolved fluorescence imaging system using a gated image intensifier; and (4) an image processing unit. In this system, the excitation source is a  $N_2$ -gas laser with a 500-ps, 337-nm excitation pulse, operating at a 25-Hz repetition rate. A conventional Olympus fluorescence microscope adapted for epi-illumination was used. The laser beam was directed into the epi-illumination port through a series of optical components (including a UV optical fiber and collimators) so as to uniformly illuminate the entire area of the 2-D samples. Fluorescence emission from the sample is directed through an objective lens to the photocathode of a gated image intensifier with additional FLI components described previously.

A FLIM using the frequency-domain method for lifetime imaging measurements of calcium in living cells has been reported.<sup>12</sup> The system was based on the FLI system mentioned in Section III.C. The FLIM has been installed on the side

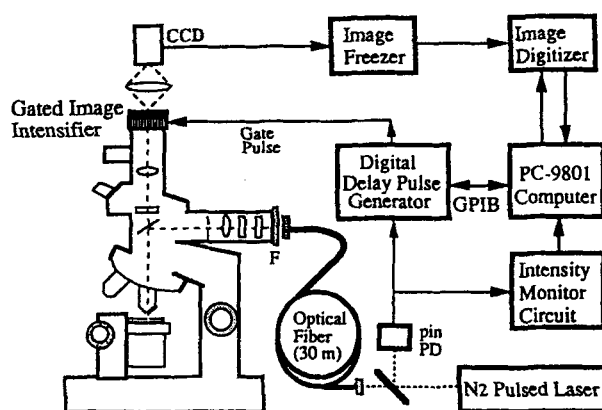


**FIGURE 13.** A time-resolved fluorescence microscopy system using a gated image intensifier.

port of a Nikon Diaphot fluorescence microscope. The microscopic sample is illuminated with an intensity-modulated light source, in this case picosecond pulses from a cavity-dumped dye laser, which are intrinsically modulated at integer multiples of the pulse rate. The excitation source is the frequency-doubled output of a Pyridine-1 dye laser, which is synchronously pumped by a mode-locked Nd:YAG laser and cavity-dumped at 3.81 MHz. The emission image is quantified using an image intensifier and slow-scan cooled CCD camera. The gain of the image intensifier is modulated at 49.53 MHz using the output of a frequency synthesizer. The output of the frequency synthesizer is phase-locked to the pulsed excitation using the same 10-MHz master oscillator for the frequency synthesizer, which also triggers the im-

age intensifier and the Nd:YAG mode-locker. The phase of the synthesizer output is varied using the digital phase shift option of the frequency synthesizer. Gain modulation of the image intensifier is at an exact integer multiple of the pulse repetition rate (i.e., homodyne detection), resulting in stationary phase sensitive images on the phosphor of the intensifier. Another FLIM has been reported using frequency-domain FLI with a wide range of temporal resolution available for measuring either delayed luminescence (milliseconds to seconds) or fluorescence (subnanosecond to hundreds of nanoseconds).<sup>68</sup> Homodyne detection was carried out on the intensifier cathode (for low-frequency homodyne detection) and the high-frequency modulation on the MCP. The system also can be operated in a heterodyne detection mode.

In conventional FLIM, it is desirable to use a broad-band light source, which allows complete tunability across the absorption bands of fluorescent species. This permits a wider choice of fluorescent probes and efficient resolution of overlapping spectral emissions by processing images measured at a series of excitation wavelengths. Various laser sources (shown in Table 5) are available for conventional FLIM with multi-line output, but offer only a limited selection

of wavelengths, especially in the UV range. N<sub>2</sub> lasers are inexpensive, but are pulsed at low duty cycle. Tunable dye lasers are available that can cover a wide spectral range; harmonic generation can give access to UV excitation. Unfortunately, only very expensive systems have a sufficiently high repetition rate.

For conventional FLIM, other problems that need to be addressed include photobleaching, detection sensitivity, and position-dependent response of the image detector. In order to improve detection sensitivity, a two-stage MCP image intensifier can be used. The position-dependent response of the image detector (which is caused by the time delay for the voltage to pass across the photocathode) can affect lifetime calculation, especially in frequency-domain FLI. It can be corrected by measurement of uniform standard samples and calibrating against these images.

## B. Confocal FLIM

Confocal fluorescence microscopy offers elimination of out-of-focus fluorescence, and excellent spatial and depth resolution allowing accurate location of the distribution of fluorescent

**TABLE 5**  
**Various Laser Sources for FLIM**

Light sources	
YAG-pumped tunable dye laser system Wavelength: 340 nm–IR Pulse width: 1–3 ps Repetition rate: 76 MHz	Coherent, Inc., Palo Alto, CA Quantronix, Smithtown, NY
Argon-ion pumped tunable dye laser system Wavelength: UV–IR Pulse width: 3–10 ps Repetition rate: 82 MHz	Coherent, Inc., Palo Alto, CA Spectraphysics, Piscataway, NJ Quantronix, Smithtown, NY
Ti-sapphire laser (Argon-ion pumping source) Wavelength: 680–1100 $\mu$ m Pulse width: 2–5 ps Repetition rate: 76–82 MHz	Coherent, Inc., Palo Alto, CA Spectraphysics Lasers, Piscataway, NJ
Excimer lasers Pulse width: 4–90 ns Wavelength: 157–700 nm Repetition rate: 150–400 Hz	Lambdaphysik, Acton, MA Lumonics, Inc., Canada
N <sub>2</sub> laser/pumped dye laser system	Laser Science, Inc., Cambridge, MA

species within unsectioned samples.<sup>69</sup> More importantly, confocal microscopy can provide 3-D information by optically sectioning the sample.<sup>70</sup> Different types of confocal microscopy, such as laser beam scanning, stage scanning, and tandem scanning, exist and allow the user to analyze the dynamic structural information of the specimen in three dimensions.

A general confocal FLIM is shown in Figure 14. The confocal FLIM is a 3-D space- and time-resolved fluorescence spectroscopy system based on stage scanning confocal fluorescence microscopy and SPC detection.<sup>71</sup> In the system, a picosecond, wavelength tunable, and high repetition rate pulsed laser system was used. 3-D lifetime imaging was obtained by scanning an XYZ stage. A confocal FLIM based on streak camera detection, stage scanning, and picosecond laser diode excitation have been commercialized by Hamamatsu Photonics Co. (tMAP-1).<sup>72</sup> Temporal resolution is better than 40 ps, and the excitation light source ranges from visible wavelengths (e.g., 400 nm using second harmonic techniques) to the near infrared (e.g., 750 nm for photoluminescence lifetime imaging). Since a streak cam-

era was used, time and wavelength information could be simultaneously detected. In a recent manuscript, an interesting fluorescence lifetime measurement system using a novel fiber optic laser scanning confocal microscopy was discussed.<sup>73</sup> However, because these instruments require stage scanning and SPC detection, they suffer from the need for long measurement times. In order to improve temporal resolution, a confocal FLIM was designed using MPC technique, which reduced the measurement time by a factor of two to three compared with SPC. This instrument was used to measure DNA information.<sup>45</sup>

Frequency-domain confocal FLIM has not been reported yet. Frequency-domain fluorescence microscopy without 2-D scanning could be constructed by combining a normal cuvette-based, frequency-domain heterodyne lifetime instrument with an epi-illumination microscope. It would be straightforward to combine laser scanning confocal microscopy and frequency-domain lifetime detection to create confocal FLIM. The laser beam can be modulated easily using an acousto-optic modulator or Pockels cell. A photomultiplier can be used for detection in which a pair of RF mixers

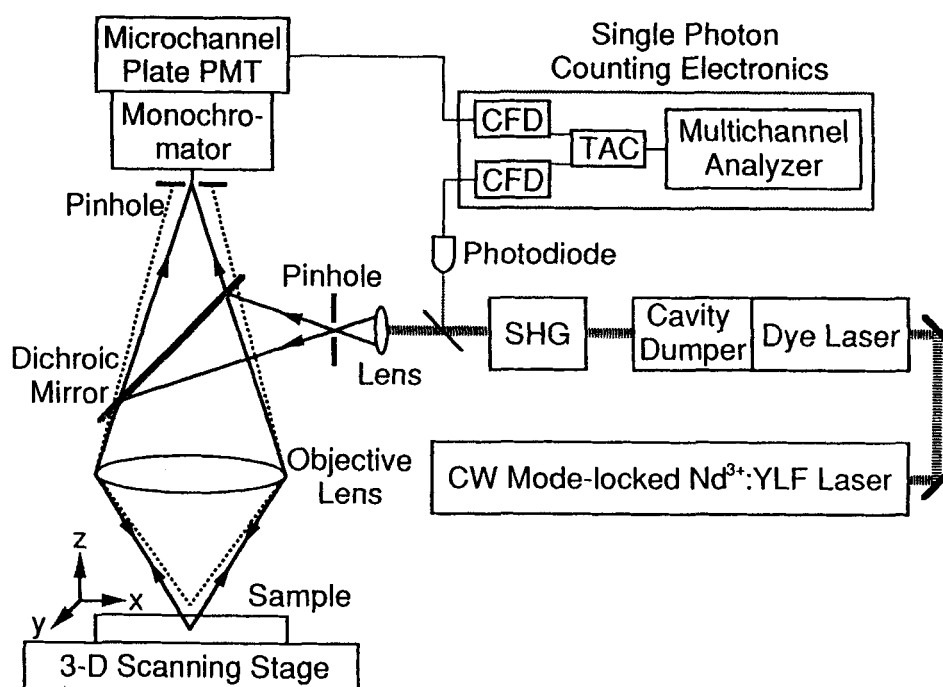


**FIGURE 14.** Schematic diagram of the three-dimensional space- and time-resolved fluorescence spectroscopic system based on a confocal microscope.

would be used to correlate the output current with RF sinusoids in-phase and in-quadrature with the excitation modulation. The lifetime image could then be accumulated in the computer as the beam scans the specimen. For this kind of confocal FLIM, a laser scanning giving  $512 \times 512$  pixels may dwell at each point only for a few microseconds if the typical total scan time of 1 or 2 s is required, so that the lifetime detection in each pixel should be completed within a few microseconds using modified hardware techniques.

A two-photon excitation confocal FLIM has been reported.<sup>74</sup> Two-photon excitation arises from the simultaneous nonlinear absorption of two red photons. Currently, this instrument is limited to providing UV excitation. Inasmuch as the rate of two-photon excitation depends on the square of the incident intensity, the resulting fluorescence is limited to the focal volume where the photon density of the focused laser illumination is high. This localization also limits photobleaching and any photodamage to the focal plane of the image.<sup>75</sup> Two-photon excitation provides depth discrimination matching confocal microscopy without requiring a confocal spatial filter; this advantage allows major simplification of the apparatus. These properties provide ideal conditions for lifetime imaging in order to characterize the submicroscopic environment of the fluorophore molecules within the specimen.

Another commercially available confocal scanning microscope, based on tandem scanning, uses non-laser sources that provide the benefit of excitation wavelength tunability. Tandem scanners illuminate and scan the sample simultaneously with many small spots of light. An advantage of the tandem scanner is that if the signal is high, the potential for real-time imaging exists. For fluorescence lifetime imaging detection, modified image-intensified detectors (e.g., gated image intensifiers) are available. To implement nanosecond time resolution for confocal FLIM with a tandem scanner, a modulated light source (e.g., deuterium lamp) could be used. Because such a modulated light source is typically two orders of magnitude less intense than that of a mercury arc lamp, the detector should be of high sensitivity and coupled to an integrating camera.

Laser beam scanning, wherein a single bright spot is scanned across the sample, has the considerable advantage in that it can be easily and inexpensively converted to confocal FLIM operation. This type of confocal FLIM is easily adapted to give qualitative decay-time contrast. However, it is not well suited to quantitative lifetime imaging unless long acquisition times are acceptable. A further difficulty with UV excitation in laser beam scanning is the design of well-corrected optics for UV work. Stage scanning, wherein the sample is scanned across the stationary laser beam, is better suited for quantitative measurements. In this type of microscope, the light beam is on-axis and the lens design is simplified, allowing easy use with UV sources. However, because of the mechanical stage scanning, the time required to obtain lifetime images would be long. Tandem scanning is a good choice for confocal FLIM where time integration is permissible. However, for tandem scanning, the excitation source is very inefficient, reducing its sensitivity. A typical scanning disc will be between 1 and 5% transmissive, and there are further optical losses in the microscopic optics. In real applications, the selection of confocal FLIM should be based on sensitivity, quantitativity, time resolution, and spatial resolution requirements.<sup>76</sup>

## V. APPLICATIONS

Applications of FLIM are based on following advantages:

1. The additional temporal (obtainable) information provides the ability to couple multi-parameter imaging of cellular structures with spectral information.<sup>77</sup> With steady-stage fluorescence microscopy, the number of spectral components that can be resolved is limited by the absorption and emission spectral overlap of each probe. The number of analytical parameters can be increased by FLIM even at the same wavelength.<sup>50</sup>
2. FLIM can avoid autofluorescence from living cells by simply distinguishing lifetime differences with increased contrast and sensitivity of the image.

3. Fluorescence lifetime probes are sensitive to numerous chemical and environmental factors such as pH, oxygen, and  $\text{Ca}^{2+}$ . FLIM can directly image the environmental and structural environment immediately surrounding the probe. In addition to providing 2-D maps of lipid order, (anisotropy), FLIM can also provide data on rotational and translational dynamics of cellular constituents.<sup>78</sup>
4. FLIM is an effective technique for quantifying the interaction, binding, or association of two types of molecules using fluorescence resonance energy transfer (FRET) spectroscopy.<sup>17,79–81</sup> Because FRET decreases in proportion to the inverse 6th power of the distance between the donor and acceptor probe, this phenomenon is effective when the donor and acceptor molecules are within 10 to 100 Å of each other. This method has the distinctive features of superior spatial and temporal resolution, high sensitivity, and applicability in complex systems.<sup>82,83</sup> FRET imaging is particularly useful in examining temporal and spatial changes in the distribution of fluorescent molecules in living cells by monitoring donor lifetime imaging.

The next section illustrates FLIM technology with examples taken from this laboratory.

### A. Calcium and Other Chemical Imaging

Fluorescence lifetime probes are equilibrium “probes” that respond to calcium concentrations independent of probe concentration and photobleaching.<sup>84</sup> It has been reported that changes in the levels of calcium induce a dramatic change in the lifetime of Quin-2 using phase-resolved FLIM.<sup>85</sup> There also has been a report published demonstrating that cellular calcium levels can be imaged by phase-resolved FLIM in the COS cell line.<sup>12</sup> While probe (Quin-2) concentration varied dramatically throughout the COS cell, the lifetime of Quin-2 probe and hence,  $\text{Ca}^{2+}$  concentration was relatively constant. FLIM eliminates the need for ratiometric measurements using UV wavelength (Fura 2)  $\text{Ca}^{2+}$ -sensitive probes. This

is advantageous, as recently nonratiometric probes for  $\text{Ca}^{2+}$ , such as calcium green, crimson, and orange, have been commercialized and could be used. These nonratiometric probes are extremely important for imaging the calcium concentration in the cells using confocal laser scanning microscopy. This is due to the limited visible excitation wavelengths available from most lasers used in confocal microscopes. This group is currently working on the measurement of growth factor-induced oscillations of intracellular  $\text{Ca}^{2+}$  using laser-scanning confocal fluorescence microscopy.<sup>86</sup> We have recently described the presence of oscillations in nuclear-free  $\text{Ca}^{2+}$  ( $\text{Ca}^{2+}_n$ ), which differ in frequency from cytoplasmic oscillations in  $\text{Ca}^{2+}_i$  in the same cell. At present, the significance or mechanisms that regulate hormone-induced  $\text{Ca}^{2+}$ -oscillatory activity are not clear. By using a confocal type FLIM, it is possible to quantitatively measure nuclear  $\text{Ca}^{2+}_n$  and cytoplasmic  $\text{Ca}^{2+}_i$  in the same cell separately using visible wavelength laser light excitation. Combining FLIM with caged compounds (e.g.,  $\text{IP}_3$ , cAMP, and DAG), it will be possible to determine the mechanisms that regulate these oscillations.

FLIM can be used to measure other types of cellular ions. The fluorescence lifetime probe can be dependent on pH, oxygen, intracellular metal ion (e.g.,  $\text{Mg}^{2+}$ ,  $\text{Na}^+$ ,  $\text{K}^+$ ), and a variety of other substances. For example, the fluorescence lifetime of the electron carrier nicotinamide adenine dinucleotide (NADH) increases after binding to proteins, and one can image the free and protein-bound NADH in cells.<sup>87</sup> Moreover, the time resolution of present calcium imaging systems is insufficient to study fast changes (e.g., receptor mediated) in living cellular calcium levels in real time.<sup>88,89</sup> Such changes are expected to be very rapid and not assessable using currently available instrumentation. Use of FLIM would enable examination of these transient calcium signal changes on a nanosecond time scale in living cells.

### B. Clinical Imaging

The availability of bioreagents, such as monoclonal antibodies and nucleic acid probes, for biomedical and clinical analytical purposes has

opened up new possibilities for the localization of proteins and nucleic acid sequences in tissues, cells, and chromosomes. For instance, fluorescently labeled antibodies and nucleic acid probes allow quantitative measurements of multiple disease markers in individual cells of patient specimens. DNA-binding fluorophores also are widely used for high-resolution banding in chromosome analysis, and luminescent labels are increasingly used for clinical immunoassays.<sup>90</sup> With the advent of genetic engineering and recombinant DNA technology, fluorescently labeled DNA- and RNA-hybridizing probes are becoming important tools for ultra-low-level detection of specific nucleotide sequences in chemical specimens. However, the use of these probes is associated with specific problems when used with microscopic detection. Sensitivity is limited by the autofluorescence of cells, fixatives, and optical lenses, and by light scatter in the microscope. Autofluorescence typically has an intensity equivalent to about 100 fluorescent molecules and a lifetime <100 ns. The contrast between fluorescence signals and autofluorescence noise can be significantly increased using phosphorescent and time-delayed fluorescent probes, which have lifetimes of microseconds and longer, allowing their emission to be detected after autofluorescence has decayed.

Several long lifetime probes have been made and are commercially available. The phosphor yttriumoxisulfide activated with europium ( $\text{Y}_2\text{O}_2\text{S}:\text{Eu}$ ) emits maximally at 620 nm and has a half-life of 700  $\mu\text{s}$ . This phosphor has strong luminescence, displays minimal photobleaching, and is not significantly influenced by pH or temperature. The phosphors  $\text{Zn}_2\text{SiO}_4:\text{MnAs}$  and  $\text{ZnS}:\text{Ag}$  emit in the green and blue, respectively, thus permitting simultaneous multiparameter measurements. The chelate 4,7-bis(chlorosulfophenyl)-1,10-phenanthroline-2,9-dicarboxylic acid (BCPDA) complexes with lanthanide ions (Eu, Tb, Dy, and Sm) and can be used to label antibodies, biotin and streptavidin. Amplification also is possible by multiple labeling. Using FLIM and long lifetime probes, background is suppressed by two orders of magnitude, providing exquisite sensitivity. Time-resolved fluorescence imaging of Eu chelate labels in both immunohistochemistry and *in situ* hybridization has been reported.<sup>91</sup>

Fluorescent Eu chelates have been conjugated to a variety of antibodies. These conjugates were used for the localization of tumor-associated antigen C242 in the malignant mucosa of human colon, localization of type II collagen mRNA in developing human cartilaginous growth plates, and detection of HPV genotypes in squamous epithelium of human cervix. Time-resolved phosphorescence and delayed fluorescence microscopic imaging also were used in studies of the structure of polytene chromosomes.<sup>44</sup> FLIM should allow both the contrast and sensitivity in clinical imaging to be dramatically increased.

### C. Plasma Membrane Fluidity, Transport, and Fusion

Many types of instrumentation have been used to investigate the average dynamic properties of cell plasma membranes including NMR, ESR, fluorescence recovery after photobleaching (FRAP), and fluorescence polarization spectroscopy. However, in all these methods, the lateral or translational diffusivities are averaged over many cells, over the entire membrane area of an individual cell, or averaged in the static time scale. Measurement of time-dependent fluorescence emission anisotropy/fluorescence lifetime of plasma membrane protein or lipid probes can provide dynamic information about plasma membrane fluidity, transport, and fusion. As there is growing evidence that membrane structure, composition, and function is heterogeneous, FLIM should provide a sensitive technique capable of obtaining data relative to both the dynamics and heterogeneous nature of membrane components related to plasma membrane fluidity, transportation, and fusion.

A streak camera-based, time-resolved microscope and its application to studies of membrane fusion in single cells has been reported.<sup>92</sup> Nanosecond lifetimes of fluorophores in plasma membrane of single living cells were measured for the observation of liposome fusion *in situ* and *in vivo*. The information about fusion of endosomes in single cells was obtained by monitoring the energy transfer signal. However, the measurements with the streak camera instrument could only be carried out at a single point in the plasma mem-

brane. Digitized fluorescence polarization microscopy (DFPM) has been used to monitor lipid order during hypoxic and anoxic injury in this laboratory.<sup>93</sup> However, this approach provides only static anisotropy measurements of lipid order. FLIM will allow us to monitor the time-dependent emission anisotropy of fluorescent fatty acids or phospholipid probes in hepatocytes during anoxic and hypoxic injury as a function of  $\text{pH}_i$  and  $\text{pH}_o$  to test the hypothesis that the activation of a pH-dependent phospholipase  $A_2$  may lead to altered lipid order and eventual weakness of the plasma membrane permeability barrier.

#### D. PDGF Receptor Activation

Platelet-derived growth factor (PDGF) is recognized as a major mitogen in serum for mesenchymally derived cells.<sup>94</sup> Recent findings indicate that PDGF exists as three isoforms (AA, BB, and AB), which bind to at least two distinct cell surface receptors ( $\alpha$  and  $\beta$ ). A currently unresolved but critical question is whether dimerization of PDGF receptors is required for biological activity. Other experiments have not yielded a definitive answer to this question. A more recent approach to determining if dimerization is required for PDGF activity would be to label the  $\alpha$  and  $\beta$  PDGF receptors with distinct fluorescent markers and use FLIM with the FRET method. This approach could be used to follow  $\alpha$  and  $\beta$  receptor movement and interactions in real time at the level of a single intact living cell. Such studies could test the hypothesis that PDGF receptor dimerization is required to elicit generation of second messengers (in particular, alterations in cytosolic free  $\text{Ca}^{2+}$ ). FRET, combined with FLIM, can provide measurements of the distance between  $\alpha$  and  $\beta$  receptors following PDGF isoform binding and the relationship of changes in separation distance or state of aggregation to increases in  $\text{Ca}^{2+}$ . The studies on the PDGF receptor interaction using FLIM should provide a more definitive and complete picture of the structural changes and intermolecular associations that occur when PDGF isoforms bind to these receptors. The same methods also can be used for understanding other types of signal transduction

processes such as the signal transduction in G protein-receptor coupling; EGF (epidermal growth factor), and its receptor interactions; and receptor-receptor interactions.<sup>95</sup>

There are many other potential applications for the FLIM using the FRET principle.<sup>96-98</sup> It should be possible to image and quantify the following: cyclic AMP in single cells,<sup>99</sup> nucleic acid hybridization in living cells,<sup>100</sup> DNA and RNA conformation changes,<sup>101</sup> activities of HIV protease enzyme,<sup>102</sup> nucleotide binding properties,<sup>103</sup> and kinetics of association between CD4 or CD8 proteins and other proteins, which play important roles in immunological T-cell activation.<sup>104</sup>

#### VI. CONCLUSIONS

Research on FLIM is in its infancy. Accordingly, the development of FLIM instrumentation remains an important issue for establishing FLIM methodology and applications. Our assessment follows:

In general, the photon counting mode FLIM exhibits high sensitivity, high temporal resolution, and low photobleaching. Inasmuch as a laser system is not necessary for this instrumentation, less expensive FLIM is possible. The SPC system is well established in both hardware and software. The MPC design has not yet gained in popularity, although it may have improved data collection efficiency and shorter measurement times for each point. However, photon counting mode FLIM based on MPC and SPC suffers the problem of long measurement time for practical applications. Photon counting using a PMT is suitable for single point or several points lifetime measurement, but not for lifetime imaging. FLIM based on a 2-D photon counting tube may change this prospect in the future. However, this type of device would be very expensive and would still require long measurement times.

Frequency-domain fluorescence spectroscopy is well established in terms of instrumentation and data analysis. Frequency-domain FLIM exhibits high lifetime resolution and is capable of multicomponent lifetime imaging; its major disadvantage is that data collection times are too long for observing dynamic cellular events. FLIM using either homodyne or heterodyne detection

with gated image intensifiers also is limited by photobleaching and position-dependent response (caused by the electronic shift within the photocathode). If a heterodyne output is obtained by using a mechanical chopper or by double modulation of the image intensifier, the time-dependent output of the intensifier contains the effects of nonlinear modulation and/or saturation. Use of a chopper also has the serious disadvantage of discarding about 95% of the light due to selective observation of a small time window (phase) of a low-frequency signal. Using an image dissector tube, it is possible to construct an FLIM based on heterodyne detection. However, for many reasons, the image dissector tube has become a less popular device in recent times. Moreover, signal integration is not possible using image dissector tubes thus limiting detection of low-level signals. Frequency-domain detection may be a good choice for a confocal FLIM. By combining established hardware for single-point, frequency-domain lifetime detection and confocal microscope, it may be possible to create a real time confocal FLIM.

Time domain FLIM using a gated image intensifier exhibits fast lifetime imaging (single exponential component), "real time" time-resolved images, and low photobleaching. By coupling two or more stages of MCPs, remarkable sensitivity can be achieved. The minimal gate width for general commercialized gated image intensifiers is about 3 ns. However, this minimal gate width is not synonymous with the minimal lifetime resolution. The shortest lifetime that can be measured using FLIM is dependent on the SNR of the system. In time-resolved fluorimetry, lifetimes comparable to 10% FWHM of the system response function can be measured. If the SNR is large enough, subnanosecond ( $\approx 0.5$  ns) lifetime imaging is possible. The capability of real time time-resolved images is useful for the measurement of nonexponential fluorescence decay phenomena. By coupling two or three gated image intensifiers to two or three emission ports of the microscope, it is possible to obtain nanosecond-scale transient time-resolved images. Using multigate sampling time-resolved images with a picosecond order pulse delay generator, it would be possible to analyze multicomponent lifetime images. However, in the case of multicomponent samples,

image processing methods need to be developed to extract individual lifetime imaging. Also, limitations exist in the sampling gate width and gating frequency (determined by the response time of phosphor screen of the gated image intensifier) for present gated image intensifier devices. With the development of high-speed image device technology, it is likely that one could improve sampling gate widths to subnanosecond levels and pulse gating frequency (presently 10 kHz) to over 1 MHz. FLIM based on the gated image intensifier will become popular in response to the aforementioned improvements.

Based on the above comparisons, we conclude that each FLIM approach has its advantage and disadvantages, and the approach chosen will be dictated by the applications. For our purpose, we are working on a hybrid type of FLIM. In this system, a two-stage MCP gated image intensifier is used for conventional FLIM. In order to improve temporal and spatial resolution, an SPC detection system is used for the confocal FLIM to detect desirable micrometer-size spot detail information and performing multicomponent analysis. Valuable insights can be gained by conventional FLIM and single-point lifetime detection on the same sample. We predict that this combination will produce optimum function for many applications.

"More powerful, less expensive, easier to operate" FLIM apparatus are the goals for future research. Future investigations on FLIM should be centered on developing instrumentation and software. With the development of laser diode technology, it would be possible to manufacture inexpensive FLIM based on laser diode excitation. Confocal FLIM could be developed for 3-D lifetime imaging. Coupling a fluorescence lifetime imaging system to a near-field optical microscope would produce a new version of microscopy allowing visualization of molecular information beyond the diffraction limit. Moreover, progress in biotechnology is another important aspect for the development of new chemical and immunological fluorescent probes for FLIM. We expect that FLIM technology will play an important role for the future of bioscience research and that as these instruments become available commercially, numerous applications will be forthcoming.



## ACKNOWLEDGMENTS

Research on fluorescence lifetime imaging systems was guided by Dr. S. Minami and Dr. T. Uchida in the Department of Applied Physics, Osaka University, Japan. Their valuable discussions and technical assistance are gratefully acknowledged. We would like to acknowledge the support from Provost of University of North Carolina at Chapel Hill (UNC), Dr. S. Bondurant, Dean of UNC Medical School, and Dr. Charles R. Hackenbrock, Chairman of UNC Department of Cell Biology and Anatomy. The work on the FLIM project was supported by grants from the National Science Foundation, the American Cancer Society, and the North Carolina Biotechnology Center.

## REFERENCES

1. Weber, G., From solution spectroscopy to image spectroscopy, in *Cell Structure and Function by Microspectrofluorometry*; E. Kohen and J.G. Hirschberg, Eds.; Academic Press: New York, 1989.
2. Wang, X.F.; Uchida, T.; Minami, S. *Appl. Fluorescence Technol., Time-resolved fluorescence image spectroscopy*. **1991**, 2, 25.
3. Taylor, D.L.; Wang, Y.-L. *Fluorescence Microscopy of Living Cells in Culture, Part B*; Academic Press: New York, 1989.
4. Tanke, H.J. *J. Microscopy, Does light microscopy have a future?* **1989**, 155, 405.
5. Jovin, T.M.; Arndt-Jovin, D.J. *Annu. Rev. Biophys. Chem., Luminescence digital imaging microscopy*. **1989**, 18, 271.
6. Menzel, E.R. *Laser Focus World, Ion-laser detection of fingerprints grows more powerful*. **1989**, 11, 89.
7. Tian, R.; Rodgers, M.A.J., Time-resolved fluorescence microscopy, in *New Techniques in Optical Microscopy and Spectrophotometry*; R.J. Cherry, Ed.; Academic Press: New York, 1991, pp. 312–351.
8. Paski, E.F.; Blades, M.W. *Anal. Chem., Analysis of inorganic powders by time-wavelength resolved luminescence spectroscopy*. **1988**, 60, 1224.
9. Hawkes, P.W., Photo-electronic image devices, in *Advances in Electronics and Electron Physics*, Vol. 74; Academic Press: New York, 1988.
10. Taylor, D.L.; Wang, Y.-L., *Fluorescence Microscopy of Living Cells in Culture: Part A*; Academic Press: New York, 1989.
11. Wang, X.F., Ph.D., *Fundamental Studies on the Time-Resolved Fluorescence Image Spectroscopy*, dissertation, Osaka University, Japan, 1991.
12. Lakowicz, J.R. *Laser Focus World, Fluorescence lifetime sensing generates cellular images*. **1992**, May, 60.
13. Houseal, T.W.; Bustamante, C.; Stump, R.F.; Maestre, M.F. *Biophys. J., Real-time imaging of single DNA molecules with fluorescence microscopy*. **1989**, 56, 507.
14. Mathies, R.A.; Peck, K.; Stryer, L. *Anal. Chem., Optimization of high-sensitivity fluorescence detection*. **1990**, 62, 1786.
15. Lakowicz, J.R., *Principles of Fluorescence Spectroscopy*; Plenum Press: New York, 1983.
16. Cundall, R.B.; Dale, R.E., *Time-Resolved Fluorescence Spectroscopy in Biochemistry and Biology*; Plenum Press: New York, 1983.
17. Herman, B., Resonance energy transfer microscopy, in *Methods in Cell Biology*; D.L. Taylor and Y.-L. Wang, Eds.; Academic Press: New York, 1989, Vol. 30.
18. Hiraoka, Y.; Sedat, J.; Agard, D.A. *Biophys. J., Determination of three-dimensional imaging properties of a light microscopy system*. **1990**, 57, 325.
19. Wilson, T.; Sheppard, C., *Theory and Practice of Scanning Microscopy*; Academic Press: New York, 1984.
20. Pawley, J.B., *Handbook of Biological Confocal Microscopy*; Plenum Press: New York, 1990.
21. Bayley, P.M.; Dale, R.E., *Spectroscopy and the Dynamics of Molecular Biological Systems*; Academic Press: New York, 1985.
22. Taylor, D.L.; Waggoner, A.; Lanni, F.; Birge, R., *Applications of Fluorescence in the Biomedical Sciences*; Alan R. Liss: New York, 1986.
23. Arndt-Jovin, D.J.; Robert-Nicoud, M.; Kaufman, S.J.; Jovin, T.M. *Science, Fluorescence digital imaging microscopy in cell biology*. **1985**, 230, 247.
24. Inoue, S., *Video Microscopy*; Plenum Press: New York, 1987.
25. Cherry, R.J., *New Techniques of Optical Microscopy and Microspectroscopy*; CRC Press: Boca Raton, FL, 1991.
26. Axelrod, D., Total internal reflection fluorescence microscopy, in *Fluorescence Microscopy of Living Cells in Culture: Part B*; D.L. Taylor and Y.-L. Wang, Eds.; Academic Press: New York, 1989.
27. Pohl, D.W., *Advances in Optical and Electron Microscopy*; C. Sheppard and T. Mulvey, Eds.; Academic Press: London, 1990.
28. Betzig, E.; Trautman, J.K. *Science, Near-field optics: microscopy, spectroscopy, and surface modification beyond the diffraction limit*. **1992**, 257, 189.
29. DiGiuseppi, J.; Inman, R.; Ishihara, A.; Jacobson, K.; Herman, B. *BioTechniques, Applications of digitized fluorescence microscopy to problems in cell biology*. **1985**, 3, 394.
30. Diliberto, P.A.; Bernacki, S.H.; Herman, B. *J. Cell. Biochem., Interrelationships of platelet-derived growth factor isoform-induced changes in c-fos expression*,

- intracellular free calcium and mitogenesis. **1990**, 44, 39.
31. Diliberto, P.A.; Gordon, G.; Herman, B. *J. Biol. Chem.*, Regional and mechanistic differences in platelet-derived growth factor isoform-induced alterations in cytosolic free calcium in porcine vascular smooth muscle cells. **1991**, 266, 12612.
  32. Lemasters, J.J.; DiGuiseppi, J.; Nieminen, A.-L.; Herman, B. *Nature*, Blebbing free  $\text{Ca}^{2+}$  and mitochondria membrane potential preceding cell death in hepatocytes. **1987**, 325, 78.
  33. Lemasters, J.J.; Chacon, E.; Reece, J.M.; Nieminen, A.L., Laser scanning confocal microscopy of living cells, in *Optical Microscopy: Emerging Methods and Applications*, B. Herman and J.J. Lemasters, Eds.; Academic Press: New York, 1992; pp 339–354.
  34. Lockett, S.J.; O'Rand, M.; Rinehart, C.A.; Kaufman, D.G.; Herman, B.; Jacobson, K. *Anal. Quant. Cytol. Histol.*, Automated fluorescence image cytometry: DNA quantification and detection of chlamydial infections. **1991**, 13(1), 27.
  35. Lockett, S.J.; Siadat-Pajouh, M.; Jacobson, K.; Herman, B., Automated fluorescence image cytometry as applied to the diagnosis and understanding of cervical cancer, in *Optical Microscopy: Emerging Methods and Applications*; B. Herman and J.J. Lemasters, Eds.; Academic Press: New York, 1992; pp 403–431.
  36. Florine-Casteel, K.; Lemasters, J.J.; Herman, B. *FASEB J.*, Lipid order in hepatocyte plasma membrane blebs during ATP depletion measured by digitized video fluorescence polarization microscopy. **1991**, 5, 2078.
  37. Wang, X.F.; Gordon, J.; Lemasters, J.J.; Herman, B. *Biophys. J.*, Plasma membrane diffusibility during hypoxic injury in rat hepatocytes measured by fluorescence recovery after photobleaching. 1992 (in preparation).
  38. Wang, X.F.; Kuo, S.; Lemasters, J.J.; Herman, B. *Opt. Eng.*, Multiple microscopic techniques for the measurements of plasma membrane lipid structure during hypoxia. **1993**, 32(2).
  39. Wang, X.F.; Lemasters, J.J.; Herman, B. *Bioimaging J.*, Plasma membrane architecture during hypoxic injury in rat hepatocytes measured by multiple fluorescent spectroscopic techniques. **1993**, 1(1,2).
  40. Wang, X.F.; Uchida, T.; Minami, S. *Appl. Spectrosc.*, A fluorescence lifetime distribution measurement system based on phase-resolved detection using an image dissector tube. **1989**, 43, 840.
  41. Wang, X.F.; Uchida, T.; Coleman, D.M.; Minami, S. *Appl. Spectrosc.*, A two-dimensional fluorescence lifetime imaging system using a gated image intensifier. **1991**, 45, 360.
  42. Lakowicz, J.A.; Szmajnski, H.; Nowaczyk, K.; Johnson, M.L. *Anal. Biochem.*, Fluorescence lifetime imaging. **1992**, 202, 316.
  43. Morgan, C.G.; Mitchell, A.C.; Murray, J.G., *Trends Anal. Chem.*, In situ fluorescence analysis using nanosecond decay time imaging. **1992**, 11(1), 32.
  44. Clegg, R.M.; Feddersen, B.; Gratton, E.; Jovin, T.M. *SPIE Proc.*, Time resolved imaging microscopy. **1991**, 1640, 448.
  45. Wang, X.F.; Kitajima, S.; Uchida, T.; Coleman, D.M.; Minami, S. *Appl. Spectrosc.*, Time-resolved fluorescence microscopy using multichannel photon counting. **1990**, 44, 25.
  46. Demas, J.N., *Excited State Lifetime Measurements*; Academic Press: New York, 1983.
  47. O'Connor, D.V.; Phillips, D., *Time Correlated Single Photon Counting*; Academic Press: New York, 1984.
  48. McGown, L.B.; Bright, F.V. *Anal. Chem.*, Phase-resolved fluorescence spectroscopy. **1984**, 56, 1400A.
  49. Morgan, C.G.; Murray, J.G. *Chem. Phys. Lett.*, A phase-quadrature correlator for the measurement of fluorescence-decay times by single-photon counting. **1991**, 179(3), 211.
  50. Wang, X.F.; Uchida, T.; Maeshima, M.; Minami, S. *Appl. Spectrosc.*, Fluorescence pattern analysis based on time-resolved ratio method. **1991**, 45, 560.
  51. vande Ven, M.; Gratton, E., Time-resolved fluorescence lifetime imaging, in *Optical Microscopy: Emerging Methods and Applications*; B. Herman and J.J. Lemasters, Eds.; Academic Press: New York, 1992; pp 373–402.
  52. Lakowicz, J.R., *Topics in Fluorescence Spectroscopy*, Vol. 1; Plenum Press: New York, 1991.
  53. Characteristics and applications of microchannel plates. Hamamatsu, Tech. Manual, RES-0795/April 1990.
  54. Application of MCP-PMTs to time correlated single photon counting and related procedures. Hamamatsu, Tech. Information, ET-03/June 1988.
  55. Chang, M.C.; Courtney, S.H.; Cross, A.J.; Gulotty, R.J.; Petrich, J.W.; Fleming, G.R. *Anal. Instr.*, Time-correlated single photon counting with microchannel plate detectors. **1985**, 14, 433.
  56. Yamazaki, I.; Tamai, N.; Kuma, H.; Tsuchiya, H.; Oba, K. *Rev. Sci. Instrum.*, Microchannel-plate photomultiplier applicability to the time-correlated photon-counting method. **1985**, 56, 1187.
  57. Iwata, T.; Uchida, T.; Minami, S. *Appl. Spectrosc.*, A nanosecond photon-counting fluorimetric system using a modified multichannel vernier chronotron. **1985**, 39, 101.
  58. Wang, X.F.; Tsuji, T.; Uchida, T.; Minami, S. *SPIE Proc. on Time-Resolved Laser Spectroscopy in Biochemistry III*, Multichannel photon-counting fluorimetric system using optical fiber dynamic memory technique. **1992**, 1640, 271.
  59. Thomas, R.S.; Shimkunas, A.R.; Manger, P.E. *Proc. 19th Int. Congr. High Speed Photo. Photonics*, Subnanosecond intensifier gating using heavy and mesh cathode underlays. 1992.
  60. Thomas, R.S.; Trevino, J. *Proc. 19th Int. Congr. High Speed Photo. Photonics*, Picosecond intensifier gating with a plated webbing cathode underlay. 1992.

61. Ameloot, J.M.; Beechem, J.M.; Brand, L. *Biophys. Chem.* **1986**, *23*, 155.
62. Berlman, I.B., *Handbook of Fluorescence Spectra of Aromatic Molecules*; Academic Press: New York, 1971.
63. Gratton, E.; Jameson, D.M.; Hall, R.D. *Annu. Rev. Biophys. Bioeng.* **1985**, *13*, 105.
64. Lakowicz, J.R.; Cherek, H. *Biophys. Chem.* **1987**, *28*, 35.
65. Spencer, R.D.; Weber, G. *Ann. N.Y. Acad. Sci.* **1969**, *158*, 361.
66. Lakowicz, J.R.; Berndt, K.W. *Rev. Sci. Instrum., Lifetime-selective fluorescence imaging using an RF phase-sensitive camera.* **1991**, *62*, 3653.
67. Dovichi, N.J. *Rev. Sci. Instrum., Laser-based microchemical analysis.* **1990**, *61*, 3653.
68. Marriott, G.; Clegg, R.M.; Arndt-Jovin, D.; Jovin, T.M. *Biophys. J., Time resolved imaging microscopy: phosphorescence and delayed fluorescence imaging,* **1991**, *60*, 1374.
69. Wilson, T.; Sheppard, C. *Theory and Practice of Scanning Microscopy*; Academic Press: New York, 1984.
70. Shaw, P.J.; Rawlins, D.J. *Prog. Biophys. Mol. Biol., Three-dimensional fluorescence microscopy.* **1991**, *56*, 187.
71. Sasaki, K.; Koshioka, M.; Masuhara, H. *Appl. Spectrosc., Three-dimensional space- and time-resolved fluorescence microscopy.* **1991**, *45*, 1041.
72. Hamamatsu tentative specification sheet:  $\tau$ MAP-1, The 2-D measurement and analysis system of photoluminescence intensity and lifetime, April/1990.
73. Ghiggino, K.P.; Harris, M.R.; Spizzirri, P. *Rev. Sci. Instrum., Fluorescence lifetime measurements using a novel fiber-optic laser scanning confocal microscope.* **1992**, *63*, 2999.
74. Piston, D.W.; Sandison, D.R.; Webb, W.W. *SPIE Proc. on Time-Resolved Laser Spectroscopy in Biochemistry III, Time-resolved fluorescence imaging and background rejection by two-photon excitation in laser scanning fluorescence microscopy.* **1992**, *1640*, 301.
75. Denk, W.; Strickler, J.H.; Webb, W.W. *Science, Two-photon laser scanning fluorescence microscopy.* **1990**, *248*, 73.
76. Morgan, C.G.; Mitchell, A.C.; Murray, J.G. *J. Microscopy, Prospects for confocal imaging based on nanosecond fluorescence decay time.* **1992**, *165*, 49.
77. McGown, L.B. *Anal. Chem., Fluorescence lifetime filtering.* **1989**, *61*, 839A.
78. Stubbs, C.D.; Williams, B.W., Fluorescence in membrane, in *Topics in Fluorescence Spectroscopy*; J.R. Lakowicz, Ed.; Plenum Press: New York, 1991; Vol. 3, p 231.
79. Forster, T. *Ann. Physik.* **1948**, *2*, 55; and in *Modern Quantum Chemistry*, O. Sinanoglu, Ed.; Academic Press: New York, 1966; pp 93–137.
80. *Biophysical and Biochemical Aspects of Fluorescence Spectroscopy*; T.G. Dewey, Ed.; Plenum Press: New York, 1991.
81. Kubitscheck, U.; Kircheis, M.; Schweitzer-Stenner, R.; Drey bordt, W.; Jovin, T.M.; Pecht, I. *Biophys. J., Fluorescence resonance energy transfer on single living cells: application to binding of monovalent haptens to cell-bound immunoglobulin E.* **1991**, *60*, 307.
82. Stryer, L. *Annu. Rev. Biochem., Fluorescence energy transfer as a spectroscopic rules.* **1978**, *47*, 819.
83. Ludwig, M.; Hensel, N.F.; Hartzman, R. *Biophys. J., Calibration of a resonance energy transfer imaging system.* **1992**, *61*, 845.
84. Keating, S.M.; Wensel, T.G. *Biophys. J., Nanosecond fluorescence microscopy: emission kinetics of Fura-2 single cells.* **1991**, *59*, 186.
85. Lakowicz, J.A.; Szmazinski, H.; Nowaczyk, K.; Johnson, M.L. *Cell Calcium, Fluorescence lifetime imaging of calcium using Quin-2.* **1992**, *13*, 131.
86. Diliberto, P.A.; Periasamy, A.; Herman, B., Distinct oscillations in cytosolic and nuclear free calcium in single intact living cells demonstrated by confocal microscopy, in *Proc. 49th Annu. Meet. Electron. Microsc. Soc. Am.*; G.W. Bailey, Ed.; San Francisco Press: CA. 1991; p 228.
87. Lakowicz, J.A.; Szmazinski, H.; Nowaczyk, K.; Johnson, M.L. *Proc. Natl. Acad. Sci. U.S.A., Fluorescence lifetime imaging of free and protein-bound NADH.* **1992**, *89*, 1271.
88. Hibino, M.; Shigemori, M.; Itoh, H.; Nagayama, K.; Kinoshita, K. *Biophys. J., Membrane conductance of an electroporated cell analyzed by submicrosecond imaging of transmembrane potential.* **1991**, *59*, 209.
89. Kinoshita, K.; Itoh, H.; Ishiwata, S.; Hirano, K.; Nishitaka, T.; Hayakawa, T. *J. Cell Biol., Dual-view microscopy with a single camera: real-time imaging of molecular orientations and calcium.* **1991**, *115*(1), 67.
90. Diamandis, E.P.; Christopoulos, T.K., Detection of lanthanide chelates and multiple labeling strategies based on time resolved fluorescence, in *Nonisotopic DNA Probe Techniques*; L.J. Kricka, Ed.; Academic Press: New York, 1992; pp 263–273.
91. Seveus, L.; Vaisala, M.; Soini, E., *Cytometry, Time-resolved fluorescence imaging of europium chelate label in immunohistochemistry and in situ hybridization.* **1992**, *13*, 329.
92. Kusumi, A.; Tsuji, A.; Onishi, S.I. *Biochemistry, Development of a streak-camera-based time resolved microscope fluorimeter and its application to studies of membrane fusion in single cells.* **1991**, *30*, 6517.
93. Florine-Casteel, K.; Lemasters, I.I.; Herman, B., Digitized fluorescence polarization microscopy of DPH and related probes in cell-size vesicles composed of gel- or fluid-phase phospholipid, in *Optical Microscopy for Biology*; B. Herman and K. Jacobson, Eds.; Wiley/Liss: New York, 1990; p 559.

94. Beckmann, M.P.; Helden, C.; Westermark, B.; Di Marco, E.; Di Fiore, P.P.; Robbins, K.C.; Aaronson, S.A. *Science*. **1988**, *241*, 1346.
95. Phillips, W.J.; Cerione, R.A., Fluorescence investigations of receptor-mediated processes, in *Biophysical and Biochemical Aspects of Fluorescence Spectroscopy*; T.G. Dewey, Ed.; Plenum Press: New York, 1991.
96. Lakowicz, J.R., *Topics in Fluorescence Spectroscopy*, Vol. 1. *Techniques*; Vol. 2. *Principles* and Vol. 3. *Applications*.; Plenum Press: New York, 1991.
97. Howie, A., *J. Microsc.*, *Future trends in microscopy*. **1989**, *155*, 419.
98. Morrison, L.E., Detection of energy transfer and fluorescence quenching, in *Nonisotopic DNA Probe Techniques*, L.J. Kricka, Ed.; Academic Press: New York, 1992; pp 312-351.
99. Adams, S.R.; Harootunian, A.T.; Tsien, R.Y. *Nature, Fluorescence ratio imaging of cyclic AMP in single cells*. **1991**, *349*(21), 694.
100. Cardullo, R.A.; Agrawal, S.; Wolf, D.E. *Proc. Natl. Acad. Sci. U.S.A.*, *Detection of nucleic acid hybridization by nonradiative fluorescence resonance energy transfer*. **1988**, *85*, 8790.
101. Griep, M.A.; McHenry, C.S. *J. Biol. Chem.*, *Fluorescence energy transfer between the primer and  $\beta$  subunit of DNA polymerase III holoenzyme*. **1992**, *267*(5), 3052.
102. Matayoshi, E.D.; Wang, G.T.; Erickson, J. *Science*, *Novel fluorogenic substrates for assaying retroviral proteases by resonance energy transfer*. **1990**, *247*, 954.
103. Shapiro, A.B.; McCarty, R.E. *J. Biol. Chem.*, *Substrate binding-induced alteration of nucleotide binding site properties of chloroplast coupling factor I*. **1990**, *265*(8), 4340.
104. Mittler, R.S.; Rankin, B.M.; Kiener, P.A. *J. Immunology*, *Physical associations between CD45 and CD4 or CD8 occur as late activation events in antigen receptor-stimulated human T cells*. **1991**, *147*(10), 3434.